ELECTRICAL, OPTICAL AND STRUCTURAL STUDIES OF SOME MIXED THIOGALLATE SEMICONDUCTORS

A THESIS SUBMITTED TO THE
UNIVERSITY OF POONA
FOR THE DEGREE OF
DOCTOR OF PHILOSOPHY
(IN PHYSICS)

by

S. T. KSHIRSAGAR, M. Sc.

SOLID STATE MATERIALS DIVISION,
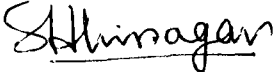NATIONAL CHEMICAL LABORATORY
POONA - 411 008 (India)
November 1976

ACKNOWLEDGEMENT

C O N T E N T S

Page

*****

CHAPTER - 1 : GENERAL INTRODUCTION

G E N E R A L   I N T R O D U C T I O N

1.1 INTRODUCTION

A distinct trend of semiconductor research in the past few years is that it has become a quantitative science with a close coordination between theory and experiment. Much of the semiconductor research in the world during the past several years has been on germanium, silicon and gallium arsenide . Of great importance to study of these semiconductors is the ability to make exceptionally perfect single crystals and to control the impurities present to a high degree. These materials have therefore served and are continuing to serve as a splendid testing ground for theoretical developments.

The most fundamental of all properties of semiconductors is their band structure. Although many semiconductors have been used in a practical way without detailed knowledge of their band structure, no one can deny that many of the more interesting and subtle developments with Ge and Si have come about since we knew the form of the energy bands. Our knowledge of the band structure of all but a very few semiconductors is very rudimentary and one of the most needed developments in the subject lies in finding more powerful methods, both theoretical and experimental, for determining the form of the energy bands

in some details. Many ternary compounds have not yet
received attention for the calculation of their band
structure.

From an experimental point of view the most
extensively studied characteristics of semiconductors are
their transport properties. Another field of research
which has contributed greatly to our understanding of
semiconductors has been a study of their optical properties.
Use of strong magnetic fields in conjunction with the
latter has added greatly to the power of technique.
These two subjects, transport and optical properties of
semiconductors, are perhaps the most important features
of semiconductor physics.

The marked success of semiconductor research in
the past decade has largely been due to the availability
in pure form and as single crystals of the materials for
investigations. Much of the early work in semiconductors
was bedevilled by non-reproducibility and uncertainty
owing to the presence of uncontrolled impurities and to
the effects of boundaries between microcrystals in the
polycrystalline samples which were generally used.

In recent years the preparation of single crystals*
of reasonable size and purity has proved to be necessary

for the study of almost all bulk and surface properties
of semiconductors as well as for most practical applications.

One may, however, exaggerate the present situation
by saying that the p-n junctions and the diversity of
phenomena discovered on pure Ge, Si and GaAs etc. cover
the whole field of semiconductors. Though several pheno-
mena in these semiconductors have been studied extensively,
there still remains much to be done for other semiconductors.
Apparently researchers' interest will be shifted to
different materials, to unexpected phenomena, to a different
kind of properties thus enriching our knowledge of
semiconductors.

1.2 USEFUL SEMICONDUCTORS

A wide variety of crystalline elements and inorganic
and organic compounds show some degree of semiconductivity,
and there are even a few vitreous or amorphous semicondu-
ctors. Apart from their use in transistors, they have a
number of other important applications (Table-1). Silicon
and germanium are the most extensively used elemental
semiconductors and a great deal of the advanced electronics
is dependent on them. Some important uses have also been
found for GaAs and other compound semiconductors utilizing
optical, thermal and electrical properties which silicon
does not possess. There are still other areas where

TABLE - 1

Semiconductor	Uses
Ge	Transistors, Diodes
Si	Diodes, Transistors, Field effect transistors, Controlled rectifiers, Integrated circuits, Solar batteries, Photocells, Nuclear radiation detectors, Stain gauges etc.
C (Diamond)	Gamma-ray detectors.
SiC	
GaP	Light emitting diodes.
$GaAs_{1-x}P_x$	
GaAs	Microwave oscillators, IR light emitting diodes, Semiconductor lasers.
CdS	Photoconductive light meters, Gamma-ray detectors.
Se	Photovoltaic light meters, Rectifiers.
InSb	Hall effect magnetometers, IR detectors.
InAs	
PbS	
PbSe	IR detectors.
PbTe	
Bi_2Te_3	Thermoelectric generators, Thermoelectric refrigerators.
Bi_2Se_3	

semiconductors have already been or will be applied and which will require a rational selection of materials with the optimum combination of properties for each individual area of technical application. Such a selection of materials can not be achieved in any way other than by the multiple investigation of large groups of substances which have semiconductor character. Germanium which belongs to the IV(A) group of the periodic table of elements crystallizes with a diamond lattice, a kind of cubic structure in which atoms have four valence electrons that form sp^3 hybridized tetrahedral bonds with four adjacent atoms making the crystal a covalently bonded macromolecule. Silicon has the same crystal structure but a large band gap, enabling devices made from it to operate at a higher temperature.

A far reaching similarity exists between these elements and the chemical compounds formed by their neighbouring elements. Many binary compounds of elements of group III(A) and V(A) (e.g. GaAs, InSb) represented by the chemical formula $A^{III}B^V$ have been found to be, in many respects (such as structure and electrical properties), similar to the elements of group IV(A). Similarly binary compounds such as $A^{II}B^{VI}$ formed by elements equidistant

from group IV(A) of the periodic table are found to have
similar structural and other properties as that of
diamond group. The striking common feature of these
compound semiconductors is that the cations form the
tetrahedral (sp^3) covalent bonding with anions similar
to that in diamond. Thus the family of these compound
semiconductors is classified as diamond-like semiconductors.

After establishing the principal properties of
$A^{III}B^V$ and $A^{II}B^{VI}$ semiconductors[1], as well as the proper-
ties of solid solutions based on these compounds, it became
clear that the next stage of the search for new semicondu-
ctors should be directed towards heterovalent ternary
compounds. Ternary diamond-like compounds are very close
electron-nuclear analogs of $A^{III}B^V$, $A^{II}B^{VI}$ and A^IB^{VII}
compounds, in respect of their composition, crystal
structure and nature of chemical bonds. One of the most
important properties of the structure of ternary compounds
is the possibility of an additional ordering compared with
the binary diamond-like compounds. In the binary compounds
cations are ordered relative to anions while in ternary
there are two different cations (or anions) and therefore
it has an additional ordering of cations (or anions)
relative to one another. Ternary compounds have many
advantages over binary ones particularly in respect of

their much lower melting points, which eventually reduces contamination during synthesis and crystal growth.

Most binary diamond-like semiconductors were predicted and synthesized by employing the suggestion of Grimm and Sommerfeld[2] that for the formation of tetra-hedral diamond-like binary compounds, the constituent elements must satisfy the following two conditions :
(1) The components of a compound should belong to group equidistant from the fourth group and (2) the average number of valence electrons per atom in the compound should be four. However, this suggestion did not help in predicting new ternary diamond-like compound semiconductors. Goodman[3] showed that the ternary diamond-like compounds can be predicted by employing what he called as "cross substitution" according to which elements from groups different from that to which the substituted atom belongs are chosen as the substituents, the condition being that the valence electron : atom ratio remains constant e.g. Ge gives rise to GaAs and ZnSe. In a compound cross-substitution can occur in two ways. It can be confined to one sub-lattice usually cationic in terms of the ionic repre-sentation e.g. In CdTe, Cd can be replaced by Ag and In to give $AgInTe_2$. Alternatively, cross-substitution can affect both sublattices simultaneously e.g. Mg_2Sn gives

rise to ternary LiMgSb. Thus III-V compounds give rise
to ternary tetrahedral structures represented by $II-IV-V_2$
whereas II-VI give rise to $I-III-VI_2$. Other ternary
compounds that can be obtained by cross-substitution are
$A_2^I B^{IV} C_3^{VI}$, $A_3^I B^V C_4^{VI}$ and $A^I B_2^{IV} C_3^V$. Many of these ternary
compounds crystallize in the tetragonal structure of
chalcopyrite.

In addition to the ternary compounds having
diamond-like structure, in which the number of cations
and anions in the compound are equal and the average
number of valence electrons per atom is four, there are
many non-equiatomic compounds having diamond-like structure.
These compounds include $A_2^I B^{II} C_4^{VII}$, $A^{II} B_2^{III} C_4^{VI}$, $A_2^{II} B^{IV} C_3^{VI}$,
$A^{III} B^V C_3^{VI}$, $A^{II} B^V C_4^{VI}$ and $A^{II} B^{IV} C_3^{VI}$. They are crystallo-
graphically similar to (diamond-group) zinc blende but
have an excess or a deficiency of some component. These
are therefore termed as defect ternary compounds. The
average number of electrons per atom in these compounds
is not equal to four but varies from 4.57 to 6.00.
According to Goryunova[4] the upper limit for the existence
of tetrahedral structures is six electrons per atom.
In spite of the fact that an enormous number of defect
ternary compounds may exist theoretically, the majority
of them have not yet been found and those which are already
known are not studied in detail.

Semiconducting ternary compounds and mixed crystals
have currently gained a particular interest due to the
possibility of having a series of materials where the
forbidden gap varies with varying of the chemical compo-
sition in a rather broad way. Furthermore, these compounds
display properties such as photoconductivity and electro-
luminescence similar to those of the traditional binary
semiconductors as far as their applied physics is concerned.
The ternary compounds $A^I B^{III} C_2^{VI}$ and $A^{II} B^{IV} C_2^{V}$ which have
chalcopyrite structure have been studied thoroughly.
However, majority of compounds of the series $A^{II} B_2^{III} C_4^{VI}$
which crystallize in defect chalcopyrite structure of
thiogallate have received very little attention.

Interest in these materials (with thiogallate
structure) is generated by their defect chalcopyrite
structures which is non-centrosymmetric (I $\overline{4}$) which
could make them useful for second harmonic generation
e.g. $CdGa_2S_4$ [5,6,10] and photoconducting applications
e.g. $CdGa_2Se_4$ [7]. However literature describing their
structure and importance as photoconductors is very scanty.
There are no systematic studies of their solid solutions,
electrical and optical properties which would provide
direct information on their band structure. Theoretical
calculations on their band structure have not yet been made.

In order to fill this gap up in the literature, at least partly, studies of structural, optical and electrical properties of these two compounds and their solid solutions are presented in this thesis. Studies on their solid solution are expected to help in understanding these properties better than it is possible by the examination of individual compound.

A review on the background literature on these two compounds is presented in the sections 1.4 and 1.5. The various physical properties of semiconductors are described in section 1.3. The section 1.6 describes the problems in crystal growth of the ternary semiconductors and the importance of the chemical transport reaction method.

1.3 PHYSICAL PROPERTIES OF SEMICONDUCTORS

Because the atoms of the crystals are in close proximity, the electron orbits around different atoms overlap to some extent and the electrons interact with each other. This interaction alters their energy and, in fact, broadens the sharp energy levels in the atoms out into a range of possible energy levels called a band. One would expect the process of band formation to be well advanced for the outer, or valence, electrons at the observed interatomic distances in solids.

At absolute zero temperature, the electrons occupy
the lowest possible energy levels with the restriction
that at most two electrons may be in the same energy
level. In semiconductors and insulators, there are just
enough electrons to fill completely a number of energy
bands, leaving the rest of the energy bands empty. The
highest filled energy band is called the valence band.
The next higher band, which is empty at absolute zero
temperature, is called the conduction band. The conduction
band is separated from the valence band by an energy gap
which is an important characteristic of the semiconductor.
In metals, highest energy band that is occupied by the
electrons is only partially filled. This condition
exists either because the number of electrons is not just
right to fill an integral number of energy bands or because
the highest occupied energy band overlaps the next higher
band without an intervening energy gap. The electrons in
a partially filled band may acquire a small amount of
energy from an applied electric field by going to the
higher levels in the same band. The electrons are accele-
rated in a direction opposite the field and thereby
constitute an electric current. In semiconductors and
insulators, the electrons are found only in completely
filled bands, at low temperatures. At sufficiently high
temperature, depending on the magnitude of the energy gap,

a significant number of valence electrons gain enough
energy thermally to be raised to the conduction band.
These electrons in an unfilled band can easily participate
in conduction. Furthermore, there is now a corresponding
number of vacancies in the electron population of the
valence band. These vacancies, or holes as they are
called, have the effect of carriers of positive charge,
by means of which the valence band makes a contribution
to the conduction of the crystal. Such a semiconductor
is called an intrinsic semiconductor. Certain impurities,
known as 'donors', can ionize readily to produce electrons
in the conduction band and the material then shows
'N' (negative) type conduction. Similarly an 'acceptor'
impurity is one which ionizes to remove electrons from
valence band so that the material shows 'P' (positive) type
conduction. Such semiconductors are called as extrinsic
semiconductor. The number and type of charge carriers
can be determined by measuring the Hall coefficient and
the mobility of the charge carriers in an electric field
can be determined from the conductivity and number of
carriers. High mobilities are always useful but the
optimum band gap depends on the use for which the device
is required.

As in case for any quantum mechanical system the
energy levels of electrons in crystals are determined by

2ND B. Z.

CONDUCTION BAND

FORBIDDEN GAP

1ST B. Z.

VALENCE BAND

$-\dfrac{\pi}{a}$ $\dfrac{O}{K\rightarrow}$ $\dfrac{\pi}{a}$

FIG.1 BRILLOUINE ZONE SCHEME.   ENERGY BAND DIAGRAM

FIRST BRILLOUIN ZONE OF A ZINC BLENDE LATTICE

FIG.2 BAND STRUCTURE OF GERMANIUM

the solution of the Schrödinger wave equation. The eigen value function $E_n(\bar{k})$ is designated as the band structure of the semiconductor. For a given n the $E_n(\bar{k})$ energy as a function of wave vector $\bar{k}$ covers a certain energy interval which is called a 'Band' or a Brillouin zone (Fig. 1).

The general structure of the energy bands of a crystal can be investigated further by a group-theoretical analysis of all its symmetry properties, i.e. the space group of the crystal. To every vector $\bar{k}$ there belong a number of symmetry operations of the point group of the crystal which leave this vector invarient. They form the group G of the vector $\bar{k}$. The group G is either a sub-group of the full point group or is identical with it; it has a finite number of irreducible representations. The $E_n(\bar{k})$ for the given $\bar{k}$ can be classified according to these representations. Therefore there are only a limited number of symmetry properties of the wave functions corresponding to an energy value $E_n(\bar{k})$. The degeneracy of an energy term is given by the dimensionality of the corresponding irreducible representation. An investigation of these questions for different $\bar{k}$ especially at points or lines of high symmetry in the Brillouin zone, results in statements about the degeneracy of different energy bands at certain points, the splitting of these degeneracies,

and the compatibilities of the different symmetry chara-
cter of the wave functions at neighbouring $\overline{k}$'s.

Fig. 2 shows as an example the Brillouin zone of
the zinc blende lattice, with characteristic points and
lines of high symmetry. Fig. 2 also shows the qualitative
structure of energy bands for the Ge lattice along the Δ
and Λ axes of the Brillouin zone i.e. the possible
connections of the energy terms of a given symmetry for
different $\overline{k}$.

The variation of electrical conductivity (σ) with
temperature in the intrinsic range is given by

$$\sigma = \sigma_0 \exp. (- E_g / 2K_B T)$$

where σ_0 is a constant, K_B the Boltzmann constant.

The thermoelectric power (θ_e) of N-type and (θ_h)
of P-type semiconductors are given by

$$\theta_e = - \frac{K_B}{e} \left[(\frac{5}{2} - S) - \frac{E_F}{K_B T} \right]$$

and

$$\theta_h = \frac{K_B}{e} \left[(\frac{5}{2} - S') + \frac{E_F}{K_B T} + \frac{E_g}{K_B T} \right]$$

respectively, where S and S' are constants and E_F is the

Fermi energy.

When both types of carriers are present i.e. for intrinsic semiconductors the thermoelectric power is given by

$$\theta = \frac{\sigma_e \ \theta_e \ + \ \sigma_h \ \theta_h}{\sigma_e \ + \ \sigma_h}$$

where σ_e and σ_h are contribution to conductivity due to electrons and holes respectively.

All semiconductors in pure state show that at a certain wavelength, generally in the near or intermediate infra-red, the absorption coefficient increases rapidly and the material becomes fairly opaque at shorter wavelength. This marked increase in absorption is called the fundamental absorption.

In an interband transition an electron is raised usually from the valence band to the conduction band by the absorption of a photon. These transitions may take place in two ways: One in which only a photon is involved in addition to photons, and the other in which energy is either supplied by the crystal lattice or given up to it i.e. one or more phonons are emitted or absorbed. The former are referred to as "direct" or vertical transitions and the latter as "indirect" transitions.
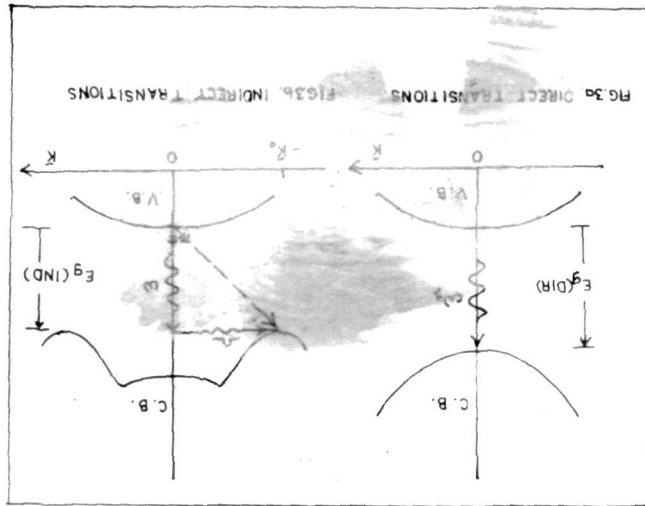
The nomenclature relevant to the energy band diagram is illustrated in Fig. (3). The energy E has been plotted in terms of the crystal momentum of wave-vector $\bar{k}$. In case of direct transitions an electron can make a transition by absorption of a photon from the valence band at $\bar{k}$ = o to the conduction band at $\bar{k}$ = o. This energy gap is direct energy gap. In case of indirect transition, an electron can make a transition from the valence band at $\bar{k}$ = o to the lowest conduction-band minimum with $\bar{k} \neq$ o by absorption of a photon followed by an absorption of a phonon (Ω) or emission of a phonon (Ω) (Fig. 3). This energy gap is an indirect energy gap.

The absorption coefficient for direct transitions as a function of energy ($\hbar w$) as calculated theoretically is given by

$$ \alpha_d = \frac{constant \ (\ \hbar w - E_g \ )^{1/2}}{\hbar w} $$

Hence the plots of ($\alpha_d \hbar w$)^2 vs $\hbar w$ should give straight lines which on extrapolation to α_d = o give the energy gap for the direct transitions.

The minimum energy for which an indirect transition may take place is given by

$$\hbar w = E_g - E_p, \text{ for absorption of a phonon } \ldots \text{ (A)}$$

$$\hbar w = E_g + E_p, \text{ for emission of a phonon } \ldots \text{ (B)}$$

The lowest value of $\hbar w$ for this type of transition is given by the equation (A) which defines the edge of the fundamental absorption band. Since E_p, the phonon energy, is generally very small compared with E_g, both types of transition affect the form of the absorption curve for values of $\hbar w$ near the fundamental absorption edge. The absorption coefficient for the indirect transition is the sum of absorption coefficients α_{1a} and α_{1e} due to the indirect transitions involving phonon absorption and phonon emission respectively. These may be expressed as

$$\alpha_{1a} = \frac{\text{const. } (\hbar w + E_p - E_g)^2}{\hbar w}$$

where $\alpha_{1a} = 0$ for $\hbar w < E_g - E_p$

$$\text{and } \alpha_{1e} = \frac{\text{const. } (\hbar w - E_p - E_g)^2}{\hbar w}$$

where $\alpha_{1e} = 0$ for $\hbar w < E_g + E_p$.

Thus it may be seen that the absorptions start at $\hbar w = E_g \pm E_p$ and are quadratic functions of the excess energy of the incident quanta over these starting values.

The plots of $(\alpha_1 \, h \, w)^{1/2}$ would therefore give rise to two straight lines with different slopes and when these lines are extrapolated to $\alpha_1 = 0$, the intercepts on the energy axis ($\hbar w$) give the values of $E_g(\text{Ind}) - E_p$ and $E_g(\text{Ind}) + E_p$. Mean of these two values would give the indirect band gap.

Since free carriers can be created in every semiconductor by some optical absorption, every semiconductor exhibits a photoconductivity. There is usually a maximum in response of photoconductivity near the absorption edge, faster surface recombination decreasing the response for "higher photon" energies and reduced absorption decreasing the response for "low photon" energies.

1.4 BACKGROUND LITERATURE ON $CdGa_2S_4$

Crystal Structure of $CdGa_2S_4$

Hahn and his colleagues[8] first prepared this compound from a mixture of binary compounds CdS and Ga_2S_3 taken in the required proportion. The product was yellowish and they investigated it by X-ray powder diffraction and reported that the compound crystallizes with space group S_4^2 and the lattice parameters $a = 5.577$ $\overset{o}{A}$, $c = 10.08$ $\overset{o}{A}$, $c/a = 1.808$. Antonov et al.[9], however, obtained higher values of the lattice parameters of the single crystals, as $a = 7.78$ $\overset{o}{A}$, $c = 10.434$ $\overset{o}{A}$. Hobden[10] analysed crushed

powder of single crystals grown by slow cooling method

and reported the lattice parameters as a = 5.54 (6) $\overset{o}{A}$

and c = 10.16 $\overset{o}{A}$. Mamedov[11] recently prepared this

compound by fusing respective components under vacuum

(1 x 10^{-4} torr) and reported that the compound had

a = 5.57 $\overset{o}{A}$ and c = 10.01 $\overset{o}{A}$.

Crystal Growth of $CdGa_2S_4$

Nitsche et al.[12,13] were the first to obtain the

single crystals of this compound by the chemical transport

reaction method using iodine as transport agent. The

size of the colourless columnar crystals was approximately

6 x 2 x 2 mm^3. The hot zone was maintained at a tempera-

ture 50°C higher than that of the cold zone (600°C).

Using the information made available by these workers

Hobden[10] grew crystals by slow cooling of the melt.

Shand[14] applied the stockbarger technique for

the crystal growth of $CdGa_2S_4$. Speeds of less than 0.6 mm

per hour only gave satisfactory results. At higher rates,

crystals invariably cracked. However, all of their

attempts to obtain colourless crystals were unsuccessful.

They obtained only yellow crystals and attributed the

cause of this colour to the non-stoichiometry which proved

difficult to rectify.

Chedzey et al.[15] examined, employing various methods, the possibility of growing large crystals for the non-linear optical applications. Their attempts to zone refining the fused material failed principally because the cracking of the silica tubes used to hold the material could not be eliminated. Other crucible materials e.g. C, Pt, were attacked by the molten sulphide. Second process involved the slow solidification of a molten charge in a manner analogous to that used by Kyropolus[16] and Cockayve et al.[17] and the loss of sulphur was prevented by a layer of molten B_2O_3[18]. But no single crystals were obtained owing to the very slow growth rates required. They also tried growth of the $CdGa_2S_4$ by the CTR technique using I_2 as the transport agent (200 mg. in 200 x 20 mm^2) with hot end and cold ends at $1000^\circ C$ and $450-550^\circ C$ respectively. This method, however, yielded them only about 3 g. of the transported material. Finally, they succeeded in growing big but yellow crystals by employing the Stockbarger technique which was similar to that used by Shand[14] and Stemple and Suehow[19]. They also studied the DTA of the thiogallates at an average heating and cooling rate of $15^\circ C/min$. DTA showed that a slow decomposition of the melt took place in an open system by the loss of volatile components. In a sealed system, the first melting point peak was a little higher

than the subsequent peaks but there was no evidence of decomposition on continued cycling through the melting point. The melting point was found to be $980^\circ C \pm 4^\circ C$ which is lower than that noted by Hobden[10] (m.p. $1050^\circ C \pm 5^\circ C$). The origin of tube breakage in $CdGa_2S_4$ was attributed to the result of strains introduced during the phase change. On the other hand, origin of tube breakage in case of $AgGaS_2$ was attributed to an anisotropic thermal expansion which was originally observed by Austin et al.[20] in case of $CuInSe_2$ and $AgInTe_2$.

Absorption Spectra of $CdGa_2S_4$

Beun et al.[13] measured the optical transmission of the single crystals of $CdGa_2S_4$ grown by the CTR method using iodine as the transport agent. They reported the values of wavelength at which α = (absorption coefficient) 500 cm^{-1} as $\lambda_{edge} = 0.358$ (μ). The dependence of α on the photon energy ($\hbar w$) was compared with various theoretical formulae. This comparison did not give convincing evidence for indirect transitions. However, value of $E_g(Ind) = 3.40$ eV obtained from the plots of $(\alpha)^{1/2}$ vs $\hbar w$ was obtained tentatively. Further, supposing that the fundamental absorption is a direct transition not forbidden at $\bar{k} = o$, value of $E_g(Dir) = 3.44$ eV was obtained from the plot of α^2 vs $\hbar w$. An appreciable absorption at the long

wavelength side was attributed to absorption due to impurities such as iodine.

Reflection Spectra of $CdGa_2S_4$

Abdullaev et al.[21] studied the optical double reflection spectra of the $CdGa_2S_4$ (and $CdGa_2Se_4$) in the 200-600 mμ region. Single crystals were prepared by the CTR method using iodine as the transporting agent. The peaks were observed at 3.58, 4.76 and 5.15 eV. The peak at 3.58 eV was attributed to the fundamental absorption arising from valence to conduction band transitions. The additional peaks were interpreted by assuming band structure of this compound similar to that of arseno-chalcopyrite e.g. $ZnGeAs_2$.

Photoconductivity of $CdGa_2S_4$

The most interesting property of these ternary chalcogenide materials is their photosensitivity. Beun et al.[13] were first to study the spectral response and other related properties of these compounds in the form of single crystals. The following data were listed for $CdGa_2S_4$. Dark resistivity (ρ_d) = 8 x 10^{13} Ω cm., light resistivity (ρ_L) = 2.5 x 10^8 Ω cm. $\rho_d / \rho_L \approx 3 \times 10^5$ and the product of mobility and life time $\mu\tau$ = 3.2 x 10^{-6} cm^2 V^{-1} and μ_H = 60 cm^2 V^{-1} sec^{-1}, response time $\approx$ 1 sec.,

photosensitivity $S \approx 9 \times 10^{-7}$ Ω^{-1} cm^2 $watt^{-1}$. The maximum photocurrent was observed at $\lambda = 358$ m μ with an additional peak at $\lambda = 410$ m μ. The former peak was correlated to the fundamental absorption edge whereas the latter was attributed to photoconductivity due to impurity such as iodine which was estimated to be 0.01% by weight. $CdGa_2S_4$ has a dependence on illumination which is close to the square root law. The voltage dependence of photoconductivity was linear.

Antonov et al.[9] observed two maxima in the photoconductivity spectral distribution curve located at 370 m μ and 470 m μ. The maximum at 370 m μ was supposed to be due to self-absorption ($E_g \approx 3.3$ eV).

1.5 BACKGROUND LITERATURE ON $CdGa_2Se_4$

Crystal Structure of $CdGa_2Se_4$

Hahn et al.[8] were the first to prepare this compound and this compound was found to crystallize with (S_4^2) space group S_4^2 having tetragonal unit cell similar to that of $CdGa_2S_4$. Lattice parameters as determined by X-ray powder diffraction were a = 5.742 $\overset{o}{A}$ and c = 10.73 $\overset{o}{A}$ with c/a = 1.87. Estimated density was 5.326 gm./cm^3 whereas the calculated density was 6.28 gm./cm^3. Subsequently this compound was studied by several workers and various values of lattice parameters obtained are as follows : a = 5.73 ± 0.006 $\overset{o}{A}$, c = 10.72 ± 0.006 $\overset{o}{A}$,

density = 5.34 gm./cm^3[22,23], a = 5.747 Å, c = 10.746 Å[24].

Crystal Growth of CdGa$_2$Se$_4$

Nitsche et al.[12,13] obtained orange-red single crystal columns (4 x 1 x 1 mm) of this compound by using CTR with iodine as the transport agent. They used a hot zone of 900°C and cold zone of 750°C. These temperatures are much higher than those which were used by Agaev et al.[24] (T_{hot} = 780°C and T_{cold} = 680°C). However Agaeve et al.[24] used concentration of iodine (8 mg/cm^3) higher than that of Nitsche et al.[12,13] (5 mg/cm^3). Though bigger crystals are feasible by method of Agaev et al., these crystals are likely to contain high concentration of iodine as impurity. It was found that band gaps for both direct and indirect transitions in CdGa$_2$Se$_4$ prepared by such methods differed considerably from the values obtained by Nitsche et al.[12,13]. Strel'tsov et al.[25] attributed this difference to the fact that crystal growth by CTR produced crystals which were not of the composition CdGa$_2$Se$_4$ but were a solid solution based on this compound. Abdullaev et al.[26] confirmed that the conditions observed in Ref. 24 for crystal growth of CdGa$_2$Se$_4$ were optimum for the stoichiometric crystal growth and showed that the crystals obtained by these conditions had 0.01% wt. accuracy in the composition

Gilevich et al.[27] studied the effect of impurities such as Cu, Ni, Pb and Ge on the CTR and on the properties of crystals. Crystals doped with Au were also synthesized by the CTR using iodine as the transport agent[21].

Optical Absorption Spectra of $CdGa_2Se_4$

Beun et al.[13] reported that for $CdGa_2Se_4$ the λ_{edge}, which is the value of wavelength at which $\alpha = 500$ cm^{-1}, was 515 mμ. The dependence of α on photon energy was compared with various theoretical formulae. As this comparison did not yield convincing evidence for indirect transitions, the tentative value of E_g (Ind) $\approx$ 2.25 eV was obtained from approximate plots of $\alpha^{1/2}$ vs hν. Plot of α^2 vs hν yielded E_g(Dir) $\approx$ 2.43 eV. Strel'tsov et al.[25] reported much lower values viz. E_g(Ind) $\approx$ 1.9 eV and E_g(Dir) = 2.1 eV for the $CdGa_2Se_4$ grown by same CTR method but by employing different conditions. Abdullaev et al.[26], however, studied the optical absorption spectrum in more detail and obtained from the plots of $\alpha^{1/2}$ vs hν and α^2 vs hν, the values of E_g(Ind) $\approx$ 2.27 eV and E_g(Dir) = 2.41 eV. The phonon energy E_{ph} = 0.04 eV was obtained from the two slopes in the plot of $\alpha^{1/2}$ vs hν. The λ_{edge} = 0.505 μ as the value of the wavelength at which $\alpha = 10^3$ cm^{-1}.

Optical absorption studies made on thin films of
$CdGa_2Se_4$[23] indicated that the E_g(Dir) = 2.15 eV and
E_g(Ind) = 1.93 eV. It should be noted that the thin films
do not contain impurities such as iodine as these were
developed by the ordinary vacuum evaporation technique.

Recently Radautsan et al.[23] measured the absorpti-
vity values (α) of p-type $CdGa_2Se_4$ (single crystal size
5 x 10 x 1.5 mm) with natural edge (112) at 80°, 178°,
218° and 300°K and were found to lie between 2.2 and 2.6 eV.
The exponential dependence of the absorption edge with the
slope depending on temperature, the stability of the
reflection maximum and photoconductivity in the near
spectral region and the high values of absorptivity ($\sim 10^4$
cm^{-1}) revealed an exciton character of the absorption.
For $\alpha \approx 10^3$ cm^{-1} the dependence of the absorption on the
photon energy was weaker. The photoconductivity and
reflection spectra for $\alpha \sim 4 \times 10^3$ cm^{-1} had a fine structure.
A strong exciton-phonon interaction and a high degree of
exciton localization were observed.

Reflectance Spectra of $CdGa_2Se_4$

Abdullaev et al.[26] studied the spectral variation
of the specular reflection and observed two peaks at 2.43 eV
and 2.52 eV. The first peak was assumed to come from the
band gap and the second peak was left without interpretation

as the band structure of this compound was not known. Their study of the diffuse reflection[29] revealed that $\Xi_g = 2.43$ eV.

Recently Abdullaev et al.[21] measured the reflection spectrum of $CdGa_2Se_4$ and found that its spectrum had a weak maximum at 2.55 eV which is close to its forbidden band width. Additional peaks at 3.87, 4.19 and 4.95 eV were interpreted by assuming the band structure similar to that of non-defect arseno-chalcopyrites.

Photoconductivity of $CdGa_2Se_4$

Studies by Beun et al.[12,13] have indicated that the $CdGa_2Se_4$ is a promising photoconductor for technical applications. They observed the highest photosensitivity ($\sim$ 3 x 10^{-4} ohm^{-1} cm^2 $watt^{-1}$) among all the ternary chalcogenides (space group I $\overline{4}$) with the decay time constant $\tau_o \sim 0.002$ sec., $\mu\tau = 7.7$ x 10^{-4} (cm^2 V^{-1}), $\rho_{dark} = 4$ x 10^{11} Ω cm., $\rho_L = 1.1$ x $10^{5}\Omega$ cm., $\rho_d / \rho_L = 4$ x 10^6. It was also observed that the photocurrent varied linearly with light intensity and the electric field applied even up to break-down voltage.

Radautsan et al.[30] presented results of spectral dependence of photoconductivity at $300^\circ K$ in the photon energy range 1.7 - 3.3 eV, with the crystal axis along the

incident light. Ohmic aluminium electrodes were deposited on the mirror smooth naturally grown surface which yielded n-type conduction with ρ_d = 10^{13} Ω cm and a relative photosensitivity ρ_d / ρ_L = 5 x 10^6 (for illumination with 10^3 lux). The photoresponse was a linear function of the illumination intensity in the range 10^{12}- 10^{15} photons cm^{-2} sec^{-1}, for all wavelengths. The photoconductivity spectrum exhibited two well resolved maxima in the range 0.46-0.70 μ. Short wavelength maximum was narrow and long wavelength maximum was broader and weaker. These were attributed to indirect and direct optical transitions from valence band to conduction band. The minimum widths of the forbidden bands E_g ($\lambda_{1/2}$) were 2.20 and 2.50 eV respectively. Beyond the direct transition edge additional peaks at photon energies $\hbar w$ = 2.81, 2.94 and 3.09 eV were observed. These were shown to arise from the electron transitions from the valence sub-bands to conduction band.

Abdullaev et al.[31] performed more systematic and detailed study of the photoconductivity and trapping and recombination processes in n-type $CdGa_2Se_4$ crystals. They observed ρ_d (at 293°K) = 2 x 10^{12} Ω cm, and relative photosensitivity ρ_d / ρ_L (at 293°K) = 3 x 10^4 which changed to > 10^6 at 200°K for 10^3 lux. Analysis of the lux-ampere characteristics and the photoconductivity relaxation curves

revealed three types of local centers, 'r' and 's' recombination centers and 't' trapping levels, in the forbidden band of $CdGa_2Se_4$. The following values were obtained for the principal parameters of the r slow-recombination centers : Energy gap from the top of the valence band, E_{vr}^T = 0.47 (thermal value) and E_{vr}^O = 0.77 eV (optical value); electron-capture cross-section S_{nr} = 1.7 x 10^{-18} cm^2, hole-capture cross section S_{pr} = 1.3 x 10^{-14} cm^2. Some of the parameters of s the fast -recombination centers (s) (S_{nr} = 2 x 10^{-16} cm^2) and of the trapping levels (concentration n_t = 2.9 x 10^{12} cm^{-3} and energy gap from the bottom of the conduction band E_{ct} = 0.33 eV) were determined. The photoconductivity spectra were recorded at $105^{O}K$ and $293^{O}K$. At $293^{O}K$ there was a maximum at λ_1 = 500 mμ due to the fundamental absorption and a maximum at λ_2 = 555 mμ due to impurity photoconductivity and a weak structure at λ_3 = 420 mμ (the corresponding wavelengths at $105^{O}K$ were λ_1 = 485, λ_2 = 530 and λ_3 = 405 mμ). The forbidden width, which was deduced from the wavelength at which the amplitude of the principal maximum fell to half its maximum value was 2.27 eV at $293^{O}K$. The impurity photoconductivity was attributed to the radiative capture of electrons by the r-centers which were singly charged acceptors. Since $S_{nr} < S_{pr}$, the r centers are the sensitizers, they capture

holes rapidly and electrons slowly. The small value of S_{nr} and the considerable difference between the values of S_{nr} and S_{pr} lead to strongly unipolar conditions and high values of the photocurrent.

Recently Abdullaev et al.[32] investigated the effect of doping on photoconducting properties of $CdGa_2Se_4$ grown by the CTR method. Their measurements revealed that Au produces n-type $CdGa_2Se_4$ and changed the ρ_d, for pure $CdGa_2Se_4$, from $10^{13} \Omega$ cm to $4 \times 10^{10} \Omega$ cm, the relative photosensitivity being $\rho_d //_L = 6 \times 10^5$ at $293°K$ and $\sim 10^7$ at $200°K$ ($L = 10^3$ lux). The photoresponse time was practically unaffected by doping ($\tau = 0.003$ sec.) and $\mu_n = 17$ cm^2 v^{-1} sec^{-1} (at $-293°K$). Photoconductivity spectra of Au-doped $CdGa_2Se_4$ crystals ($6 \times 2 \times 0.5$ mm) were recorded at $293°K$ and $105°K$. A maximum at $\lambda_1 = 500$ mμ (at $293°K$) was attributed to fundamental absorption. Two maxima at $\lambda_3 = 960$ mμ and $\lambda_2 = 635$ mμ due to impurity photoconductivity were observed alongwith a fine structure near $\lambda_4 = 420$ mμ (at $105°K$ the corresponding wavelengths were $\lambda_1 = 485$, $\lambda_2 = 600$, $\lambda_3 = 940$ and $\lambda_4 = 405$ mμ). The forbidden band width of 2.27 eV was derived from the mid point of the principal photoconductivity maximum. The λ_2 maximum was related to Au impurity which was intentionally doped. The density of trapping levels and their energy separation from conduction band were, $n_t = 6.7 \times 10^{13}$ cm^{-3}

and $E_{ct} = 0.26$ eV respectively. The following parameter values were obtained for Au-doped $CdGa_2Se_4$: $E_{vr}^T = 0.51$ eV, $S_{pr}/S_{nr} = 2.3 \times 10^5$, $E_{vr}^O = 0.91$ eV at 105°K. By assuming that the impurity photoconductivity maxima λ_2 and λ_3 were due to the ionization of the r' and 's' recombination centers, their energy gaps separating these centers from conduction band were deduced from the long wavelength edges of the impurity photoconductivity at points where the sensitivity fell to 0.1 of the maximum value. Such calculation lead to $E_{cr}^{(o)1} = 1.53$ eV, $E_{cs}^{o(1)} = 1.17$ eV at 105°K and consequently to $E_{vr}^{o(1)} = 0.82$ eV and $E_{vs}^{o(1)} = 1.18$ eV at 105°K. The behaviour of the Au-doped $CdGa_2Se_4$ was much similar to undoped $CdGa_2Se_4$ and that the Au enhanced the photosensitivity. It was concluded that in Au-doped $CdGa_2Se_4$, the r-centers were in the form of a group of acceptor levels formed by the Au-impurity atoms and by the deviations from the stoichiometric amounts of selenium which occurred during growth.

Thin Films of $CdGa_2Se_4$

Tyrzin and Tyrzin[24] studied the photoconductivity spectrum of thin films of $CdGa_2Se_4$ prepared by ordinary vacuum evaporation of a massive specimen. These films displayed photoconductivity immediately after preparation and before any additional treatment. After annealing in

air for 20 minutes at 150°C the photoconductivity increased by two orders of magnitude. The spectral dependence of the photoconductivity was an unsymmetrical curve with a flatter edge on the long wave side. The photoconductivity maximum was at 560 m u. The temperature dependence of the electrical conductivity in air and vacuum gave activation energy 2.18 eV which was higher than that of direct (2.15 eV) and indirect (1.93 eV) band gaps.

1.6 PROBLEMS IN CRYSTAL GROWTH OF TERNARY SEMICONDUCTORS AND THE IMPORTANCE OF THE CHEMICAL TRANSPORT REACTION

The most critical step in preparing solid state devices is the structural and chemical control during crystal growth. Control of crystal growth and the understanding of growth processes requires consideration of the liquidus curve and the equilibrium pressures of the various vapour species along the liquidus curve. When the information on the phase diagrams is available, crystal growth may be accomplished from the melt by employing one of the three basic methods viz. (1) floating zone[33], (2) horizontal Bridgman and (3) the Czochralski technique. These methods have been successfully used for the large area crystal growth of elemental as well as many binary compound semiconductors[34]

Phase diagrams of most of the ternary systems, in which ternary semiconducting compounds with the tetrahedral coordination are formed, have not yet been investigated. Luzhnaya et al.[35] pointed out that the nature of the phase diagram of a ternary system must be taken into account in the selection of synthesis method because the available published data suggest that ternary compounds frequently melt incongruently. This has highly impeded the crystal growth of ternary compounds by applying the traditional melt growth methods. Furthermore, crystal growth from the melt becomes exceedingly difficult if applied to materials having high melting points. Additional difficulties arise if compounds are to be grown which show appreciable dissociation (e.g. GaAs 1 atom. pressure at 1230°C, GaP 36 atom. pressure at 1550°C) at their melting or which melt only under elevated pressure (e.g. CdS). It has been shown that in order to prevent the dissociation of a compound it is necessary to establish a vapour pressure of the volatile element equal to the dissociation vapour pressure of the compound at its melting point[36]. When the vapour pressure of the volatile components in total system exceeds the dissociation pressure, the compound melts congruently but the melt obtained contains an excess of the volatile component and is not stoichiometric. When the vapour pressure of the volatile component

is too low the compound melts incongruently, i.e. it decomposes into a liquid enriched with non-volatile component and a vapour of the volatile component. Any deviation of the composition of a ternary compound from the stoichiometric ratio may affect very considerably its semiconductor properties e.g. $CdIn_2S_4$ prepared under vacuum had resistivity of 1 Ω cm whereas the one prepared under 5 atm. pressure of sulphur had resistivity 10^7 Ω cm.

Another factor which complicates the direct synthesis of some ternary compounds is their polymorphism. It has been established that, e.g. the compounds $CdSnAs_2$ and $ZnGeAs_2$, which have the chalcopyrite structure at low temperatures, undergo a polymorphic transition to the zinc-blende structure near the melting point[37]. In this case thermograms show an additional thermal effect and the zinc-blende lattice parameter assumes an intermediate value between the parameters a and c/2 of the chalcopyrite structure. It may be assumed that the large number of cracks in ingots of $CdSnAs_2$, prepared by direct synthesis from elements is not only due to a difference between the thermal coefficients along a and c directions of the chalcopyrite structure but also due to a polymorphic transition.

To obtain single crystals of materials, which have high melting points and are susceptible to dissociation, usually vapour phase methods are used. The polycrystalline

starting material is sublimed either in vacuo or in a stream of a carrier gas or the vapours of its constituents are reacted in a crystallization chamber. The temperature required for these processes are high in the vicinity of the sublimation point - and they have to be closely controlled, in order to avoid polynucleation by surpassing the usually small supersaturation range. If the process is carried out in a closed system because oxygen has to be excluded, the limiting temperature is usually given by the softening point of quartz. If inert carrier gases are used the control of their flow and the geometry of the arrangement pose additional problem.

Nitsche et al.[12] devised a method for crystal growth from the vapour phase which works well below the sublimation point of the material involved. They named the method as chemical transport reaction . In this method the solid, of which crystals are t) be grown, is sealed into a suitable evacuated container together with a certain amount of a so-called "transporting" agent (mostly a halogen or a hydrogen halide). The container is then brought into a temperature gradient and hence the solid is led into a chemical reaction with the gaseous agent. The gaseous products of the reaction flow as a result of the concentration gradient established with their formation and thus arrive in a region where the

temperature is lower (or~~higher~~). Owing to the change in temperature, the original reaction is driven in the opposite direction and hence the solid is precipitated out and crystallizes in the latter region. This technique involves therefore always at least two temperature regions, a "hot" zone (at temperature T_H) and a cold zone (at temperature T_C) and makes use of a gaseous "solvent" which is responsible for the transport of solid from one zone to the other.

Nitsche et al.[12] discussed this method at length and established the following requirements to be observed if the transport reactions are to be used for the crystal growth :

1.   The rate of transport should not be higher than the rate of growth of crystals which act as seeds.

2.   The phenomenon of polymorphism should be taken into account in the selection of the crystallization temperature.

3.   The crystallization zone should not be too small in order to prevent the formations of polycrystalline aggregates.

4.   The temperature distribution in the crystallization zone should be uniform.

5.   In those cases when the transport takes place by convection, crystals with well developed faces are obtained.

6.   A smaller temperature difference is sufficient when ampules of large diameter are used.

CTR method has been used successfully in the preparation of crystals of many ternary chalcogenides of the $A^{II}B_2^{III}C_4^{VI}$ type. By using this method, mixed crystals of solid solutions of $GaAs_{1-x}P_x$[38] ternary chalcopyrites e.g. $ZnSiAs_xP_{2-x}$[39] and $CuGaS_{2-x}Se_x$[40] have been grown. We have therefore employed this method for the crystal growth of the series of compositions $CdGa_2S_{4(1-x)}Se_{4x}$ (x = 0.0, 0.25, 0.50, 0.75 and 1.0).

*****

CHAPTER - 2 : EXPERIMENTAL TECHNIQUES

In this chapter the details of the preparation,
crystal growth and the experimental techniques used for
the measurement of various properties of the series of
compounds $CdGa_2S_{4(1-x)}Se_{4x}$ (x = 0.0, 0.25, 0.50, 0.75
and 1.0) are given.

2.1 PREPARATIONS

Spectroscopically pure samples of S, Se, Cd, Ga,
In etc. were taken for the preparation of all compounds
under investigation. The simplest method of preparing
the compound semiconductors is by direct synthesis from
the elements. The elements were all weighed correctly to
the fifth decimal place using a Mettler balance. In order
to avoid dissociation at their melting points, excess of
volatile component (usually 0.1 mol. %) was used. For
carrying out the reactions in oxygen free or vacuum,
transparent silica tubes were used. A piece of transpa-
rent silica tube of 6" in length and diameter 12 mm ID
and 15 mm OD was fused to a B-14 M-joint and closed at
another end. For each reaction fresh transparent silica
tubes were used.

Before introducing the weighed quantities of the
constituent elements, the silica tube was cleaned using
the following steps : (i) washing initially with hot water,
(ii) heating for one hour with a mixture 50:50 (concentrated)
HNO_3 and 40% HF , (iii) the removal of acids by washing
in boiling water, and (iv) removal of adsorbed gases by
heating in vacuum, (v) pyrolitic deposition of graphite
inside walls of the ampoule. The weighed quantities were
transferred into the ampoule through the B-14 M-joint and
then a narrow constriction was made at the top portion of
the ampoule so that it could be sealed off easily. During
the process of making the constriction the materials
containing end of the ampoule was kept in the mixture of
ice and salt. This cooling was necessary in order that
materials inside should not get oxidised. The ampoule
was then attached to the vacuum system via a B-14 F-joint
and evacuated. The evacuation was carried out for 5-6
hours and when a vacuum of 10^{-5} to 10^{-6} mm of Hg was
reached the tube was sealed off at the constriction.

A conventional vacuum unit that was used for evacua-
tion of the ampoule is shown in the Fig. 4. All the
traps were maintained at the liquid air temperature.

The sealed ampoule was then enclosed in another
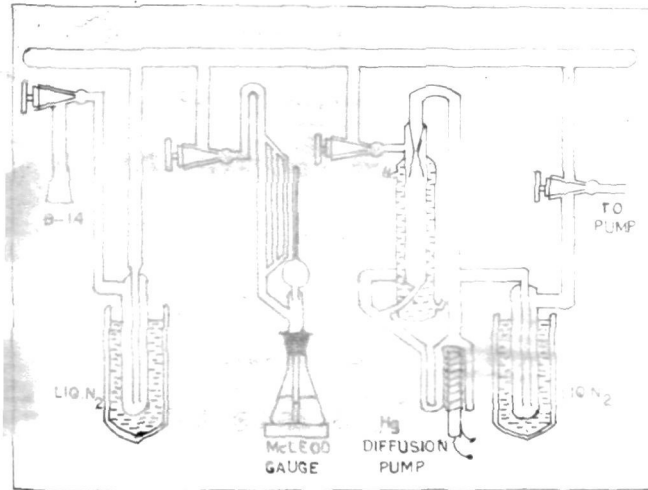empty quartz ampoule and was sealed after evacuation to
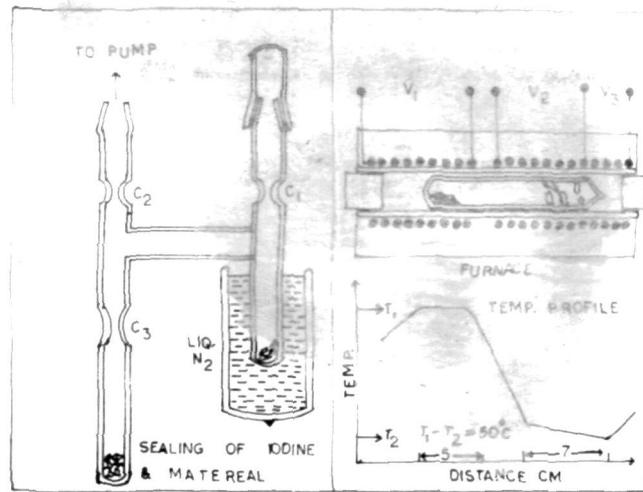
FIG.4 CONVENSIONAL VACUUM UNIT

FIG.5 APPARATUS FOR CRYSTAL GROWTH.

10^{-5} to 10^{-6} mm of Hg. This enclosing container was
necessary because while cooling, (after the melting was
carried out) gradually to room temperature the quartz
ampoule containing the charge was found to crack frequently
at temperatures of about 500°C. This cracking is thought
to occur due to different coefficients of expansion of
the solidified charge and the quartz tube. The outer
quartz container saved the hot ingot from exposure to
atmospheric oxygen.

After evacuation and sealing, the ampoule was
heated in a tube-type furnace which can attain a maximum
temperature of 1200°C and the control was $\pm$ 10°C. For
melting of all the compounds of the series the following
heating cycle was used :

$$\text{Room Temperature} \xrightarrow{\text{2 hrs}} 250^{O}\text{C} \xrightarrow{\text{4 hrs}} 600^{O}\text{C} \xrightarrow{\text{24 hrs}}$$

$$600^{O}\text{C} \xrightarrow{\text{16 hrs}} 1050^{O}\text{C} \xrightarrow[\text{rocking}]{\text{12 hrs}} 1100^{O}\text{C} \xrightarrow{\text{24 hrs}} \text{R.T.}$$

The ingots, which were polycrystalline, were then
removed and crushed to powder with an agate mortar and
pestle. The finely powdered mass was then analysed by
X-ray powder diffraction at room temperature, using a
14 cm Debye-Scherrer camera and $Cu\text{-}K_{\alpha}$ radiation filtered
through Ni-foil. The patterns were carefully checked for

the formation of homogeneous single phase solid solution and that there were no extra lines due to unreacted materials.

2.2 CRYSTAL GROWTH

The crystals of the series $CdGa_2S_{4(1-x)}Se_{4x}$ were grown by employing the chemical transport reaction method. The principles of this method have been described earlier. Iodine was used as the transporting agent. The compounds (polycrystalline) which were prepared by using the procedure described in the previous section were used as the starting materials instead of the elements directly. Previous workers have used the elements as the starting material. A charge of 10 gm was introduced into the quartz tube (of inner diameter 12 mm and length 15 cms.) (Fig. 5) which was fused to a B-14 M-joint. Dry pure iodine crystals, approximately 5 mg./cc., were introduced in the side tube through the constriction 'C_1' and immediately the constriction 'C_1' was sealed. (A P_2O_5 connected trap was kept between the vacuum unit and the ampoule, not shown in the diagram). Then the iodine containing tube was kept dipped in liquid air and the whole assembly was evacuated for 4-5 hours till the vacuum of 10^{-5} to 10^{-6} mm of Hg was reached. Then the constriction at 'C_2' was sealed and the quartz assembly was separated from the

vacuum unit. Then the flask containing liquid air was
removed from the iodine containing tube (T_1) to the
charge containing tube (T_2) and by occasional warming of
the iodine containing tube, (T_1), the iodine was distilled
into the charge containing tube (T_2). After all the
iodine was transferred to the T_2 end, the constriction
'C_3' was sealed off and the ampoule was separated from
the rest of the assembly.

Thus evacuated and sealed ampoule containing the
polycrystalline charge and iodine was then slowly inserted
in a tube-type furnace (Fig. 5) where a desired tempera-
ture gradient was already set up. The tube furnace was
made out of a quartz tube of inner diameter 13-14 mm and
consisted of three windings. By adjusting the electrical
power through these windings the desired temperature
gradient was obtained. The end temperatures were maintain-
ed constant using variacs and stabilized power supply.
Various end temperatures and gradients were tried till we
obtained homogeneous, good quality and uniformly coloured
crystals in every batch. Generally, the transport of the
whole charge took place in a duration of 4-5 days. After
this duration, the end from the hot end was cooled rapidly
to room temperature whereas the end containing the crystals
was slowly cooled (50°C/hour) to room temperature. Then
the crystals which were grown on the wall were removed from

the tube and were washed in dry alcohol by using ultrasonic cleaner. This was necessary to remove any free iodine deposited on the crystals. Then the crystals were dried in vacuum and stored in a completely blackened dessicator under vacuum. The various parameters that were optimized for the crystal growth of the compounds of the series $CdGa_2S_{4(1-x)}Se_{4x}$ are given in Table-11 in the next chapter.

A few crystals of each batch were crushed to powder with an agate mortor and pestle. X-ray powder diffraction patterns were taken to check their approximate composition. Laue-back reflection photographs were taken for the large well developed faces by using the 14 cm UNICAM camera and Cu-K radiation.

2.3 X-RAY DIFFRACTION

The various methods of X-ray diffraction used to study the various crystallographic parameters are described in the following:

The Debye-Scherrer method

This method was used to identify the formation of the single phase composition. A 14 cm. Debye-Scherrer camera was used where the film was kept fixed and the sample in the form of a powder coating on glass fiber was allowed to rotate in the CuK radiation filtered through Ni-filter. The values of Bragg angle θ for

various diffracted beams were determined by measuring the maximum diameter of the Debye rings. If $2S$ is the maximum diameter of a ring and R is the radial distance from specimen to film, then the angle θ in radians is $S/2R$ and in degrees the angle 57.30 times this. The d-values of the interplanar spacings were obtained from the "Tables for conversion of X-ray diffraction angles to interplanar spacings" NBS Applied Mathematics Series, 10 (1950).

The Laue-back reflection method

This method was used to identify the well developed morphological faces of the crystals. The single crystal was held stationary in a beam of Cu unfiltered radiation coming through the pinhole placed at the center of the film. The face of the crystal was every time maintained perpendicular to the beam. The back-reflected beams were recorded on the film. Laue patterns reflect the symmetry of crystal when a particular symmetry element is allowed to coincide with the beam e.g. when the X-ray beam is directed parallel to a four-fold axis of symmetry the pattern will have four-fold symmetry about the central point.

The Rotating Crystal Method

This method was used to determine the identity of unit lengths along the edges of the crystal. For this purpose, the selected edge of the crystal was allowed to
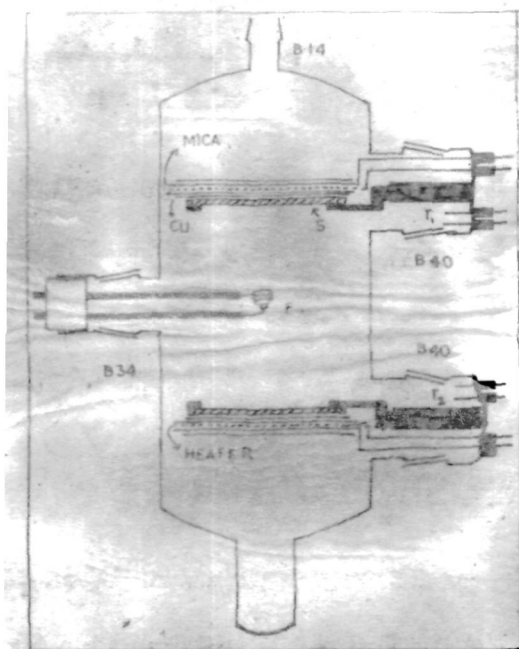
FIG. 6. VACCUM EVAPORATION GLASS UNIT.

coincide with the rotation axis. The CuK_α radiation
filtered through Ni foil was used. The orientation of
the crystal was adjusted till the reflections were arranged
in parallel layers symmetrically placed about the central
line. A unit length along the rotation axis, say $|\bar{r}|$,
was then obtained from the relation

$$ |\bar{r}| = \frac{n\lambda}{\cos \alpha_n} $$

where n is an integer, α_n is the angle of diffraction,
λ is the wavelength. α_n was determined by $\cos \alpha_n = \jmath_n/R$,
R being the radius of camera, $\jmath_n$ being the distance
of the n-th layer from the central line.

2.4 PREPARATION OF THIN FILMS

Thin films of the compounds $CdGa_2S_4$ and $CdGa_2Se_4$
were prepared by using a glass vacuum evaporation unit
as shown in Fig. 6. About 200 mg. of the compound was
placed in a conically wound tungsten filament which was
introduced through M-F joint B-34. Thoroughly cleaned
substrates mainly sodium chloride (100), quartz and
glass (optically flat) were tightly held in a substrate
holder (SH). In general substrates were placed approxi-
mately 8 cm. above the evaporation source. The substrate
holder containing substrates and substrate heater was

introduced in the vacuum unit through M-F joint B-40. The system was evacuated through the B-14 joint fused at the top. In the beginning substrates were heated to desired temperatures and then when the vacuum reached 10^{-5} to 10^{-6} mm of Hg the filament was heated slowly till the characteristic colour of the material on the substrates appeared. For both the materials, the evaporation took place just $50^{\circ}C$ below the melting point of the compounds. Thickness of the films was measured by weight method. Several temperatures of the substrate as well as those of filament were tried.

2.5 ELECTRON DIFFRACTION

Most applications of electron diffraction involve the identification of specimens in thin film form. When a stream of electrons strikes a crystal it behaves as if it were a train of waves and produce the patterns analogous to X-ray diffraction. These patterns provide the same kind of information that X-ray diffraction provides for thicker layers viz. the identification of the phase in the layer, the crystal structure of the material in the layer, the approximate grain size in the layer and the orientation present.

In the present study electron diffraction camera used was of cold cathode type[41]. All specimens were examined by transmission technique after removing deposited films from the NaCl faces. In order to find out the d-values of different reflections the graphite ring ($11\bar{2}0$ which has d-value = 1.230 $\overset{o}{A}$) was used as standard. The reflections on the pattern are given by the approximate relation

$$2rd = 2L\lambda \, ,$$

where $2r$ is the distance between the symmetrically placed reflections (or diameters of the rings in case of polycrystalline sample), d is the interplanar spacing, L is the distance from specimen to photographic plate, λ is the wavelength. The value of L λ was obtained for the every pattern from the standard graphite line ($11\bar{2}0$).

2.6 OPTICAL ABSORPTION

Specimen Preparation and Measurements

Single crystal specimens for optical absorption were prepared by waxing the crystal with its naturally grown face with holder plate and grinding the rest of the part by using SiC-abrasive papers of various grades ranging from 300, 400, 600. Finally the ground face was

polished by rubbing slowly on a teflon sheet in presence of a drop of 5% solution of conc. $HNO_3:HF(40\%)::50:50$ and then washed clean in an ultrasonic cleaner. In general the crystals were ground to thickness between 50 μ to 200 μ. Thickness was measured by weight method.

Optical absorption measurements were made by using Unicam SP500 Spectrophotometer and Perkin-Elmer 300 which permitted use of wavelength range from 200 millimicron to 1000 millimicron and optical density only upto 3. This allows the absorption measurements by normal incidence. If α is the absorption coefficient, R the reflectance and I_t the transmitted intensity, then for a given sample thickness 'd', the absorption may be determined from

$$I_t = (1 - R)^2 e^{-\alpha d}$$

Then α can be found simply from the transmission through two samples of different thickness without the knowledge of reflectance (R), provided the reflectivity of both samples is the same i.e.

$$I_{t_1} = I_o (1 - R)^2 e^{-\alpha d_1}$$

and
$$I_{t_2} = I_o (1 - R)^2 e^{-\alpha d_2}$$

$$\frac{I_{t_2}}{I_{t_1}} = e^{\alpha(d_1 - d_2)}$$

or,

$$\log \frac{I_{t_2}}{I_{t_1}} = \frac{\alpha(d_1 - d_2)}{2.303}$$

2.7 TWO PROBE METHOD FOR D.C. ELECTRICAL CONDUCTIVITY MEASUREMENTS

The major problem to be overcome in measuring bulk resistivity using applied metallic contacts is the resulting contact resistance which may be much larger than the bulk resistance of the sample. The 4-point probe method is most commonly used to avoid these barrier effects. However, when the crystals are too small to satisfactorily attach leads for 4-terminal measurements, an alternative (method) for electrical resistance measurements is to use two-terminal method based upon the characteristics of readily available electrode materials such as Ag-paste, plated Ni, In-Hg, In-Ga, Sn-Ga eutectics. Properties of metal-semiconductor contacts have been studied by many investigators[42-45] and reviewed by Henish[46]. Herman and Higier[47] studied in detail the resistivity measurements by a two-terminal method and found that In-Ga and Sn-Ga (liquid) alloys are suitable for most of the semiconductor materials. In-Ga and Sn-Ga electrodes have

FIG. 7. BLOCK DIAGRAM OF ELECTRICAL CONDUCTIVITY APPARATUS
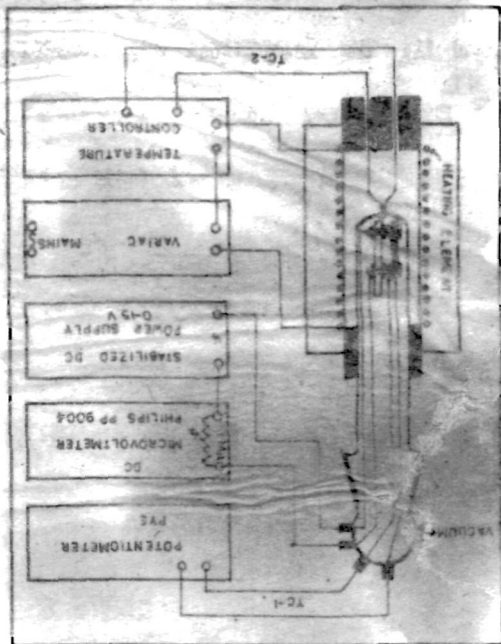
very low work functions[48] and hence show very slight
barrier (essentially Ohmic). Occasionally, however, on
the first temperature cycle the In-Ga or Sn-Ga cease to
wet one or more small portions of the semiconductor
crystals. Such a problem can be solved by heating the
sample to the peak desired temperature on a quick preli-
minary run. The contact then becomes stable for actual
measurements.

Before applying the contacts, the crystals were
lapped to provide two parallel surfaces by waxing the
naturally grown face with the holder plate. Crystals were
then ultrasonically cleaned in pure benzene and were
etched in a 1:1 mixture of 10% HNO_3 and 40% HF in water.
Finally the crystals were washed in distilled water and
dried in vacuum. In-Ga eutectic contacts were applied
on both ground surfaces by rubbing an In stick together
with a very small drop of Ga. The crystals were then
annealed in vacuum (10^{-4} mm of Hg) at $300^{\circ}C$ for 10-20
minutes.

Sample holder used for the measurement of resistance
at various temperatures was enclosed in a quartz tube
with B-34 M-F joints (Fig. 7). Two terminals (1,2) of
the metallic electrodes and two terminals (3,4) of the
chromel-alumel thermocouple were taken out through the

side tubes fused to the female joint and were made vacuum tight by filling epoxy resin in the gaps. The evacuation of the quartz tube was achieved by connecting the B-14 M-joint to the conventional vacuum unit (Fig. 4). Temperature of the sample was varied by heating the quartz tube-part containing the sample holder in the furnace (F). Stainless steel enclosure was provided for shielding the sample from external noise sources during the measurement of the resistance. In order to avoid the shorting of the metallic electrodes saphire base was used as shown in Fig. 7. The graphite slices (spacers) were used to protect deterioration of the gallium contacts due to reactions with the metallic electrodes at high temperatures.

The temperature of the sample was measured by measuring the thermocouple voltage by means of a precision portable potentiometer and was maintained constant for 10-15 minutes by using a variac and a stabilized A.C. power supply for the tube furnace. Resistance was then read as described below.

The dark resistance of the crystals was of the order of 10^{12} to $10^{13} \Omega$. A high sensitivity Philips PP9004, D.C. Microvoltmeter was used to measure the resistances. The apparatus and circuit used to measure the resistance is shown in Fig. 7. The Philips PP9004 D.C. Microvoltmeter is a versatile transistorized

vibrating reed electrometer amplifier. It can be used for making direct voltage measurements from $10\,\mu V$ to 1000 V. The polarity of the measured voltage is shown automatically by a moving coil indicator. The input resistance ($10^6\,\Omega$) of PP9004 is very accurately known. It can therefore be used for measuring very small currents (10^{-11} amp. upwards) and insulating resistances (using external voltage source). An internal calibration voltage is connected to the instrument in one of the positions of the range selector switch.

The unknown resistance is connected in series with an external stabilized voltage source of known value and the current through it is measured by PP9004. Let,

V_1 = external applied voltage,

i = current in the circuit,

R_1 = input resistance of PP9004 ($= 1\,M\Omega$),

V_2 = Voltage measured on PP9004,
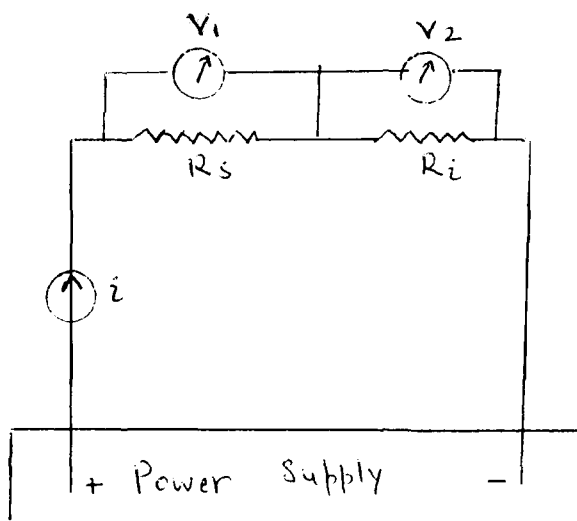
R_s = Sample resistance.

Then

$$i = \frac{V_1}{R_1 + R_s} \quad \text{and} \quad i = \frac{V_2}{R_1}$$

therefore,

$$\frac{V_1}{R_1 + R_s} = \frac{V_2}{R_1}$$

or $\quad R_s = V_1 - V_2 / V_2 \cdot 10^6$ Ohm.

For resistances in the range 10^{11} to 10^{13} Ω ,
V_1 was kept equal to 100 volts which was obtained by
using a stabilized D.C. power supply and for range 10^6 to
10^{11} Ω , V_1 was kept at 10 volts.

2.8 TH.RMOEL.CTRIC POWER MEASUREMENTS

The t.e.m.f. measurements were impeded mainly due
to the high resistivities of the crystals. However,
Burr-Brown electrometer (operational I.C.) amplifiers
model 3431 J/K, which are designed for measured of
submillivolt signals from very high source impedance
$(10^{14}$ Ω), allowed the measurements without any error
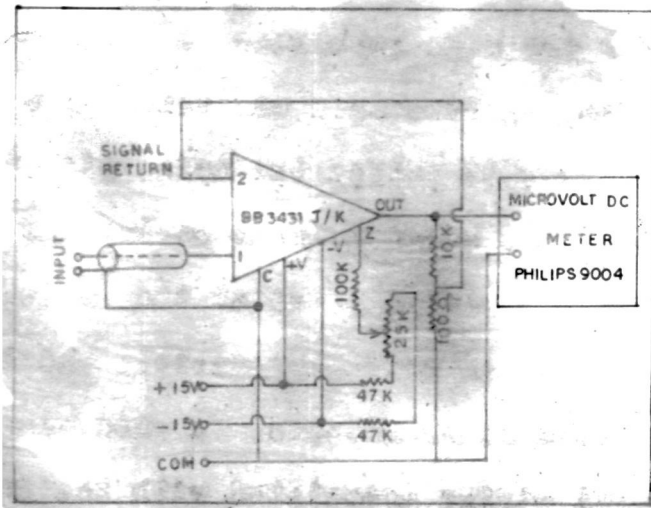upto 10^8 Ω . The circuit used to measure the t.e.m.f.
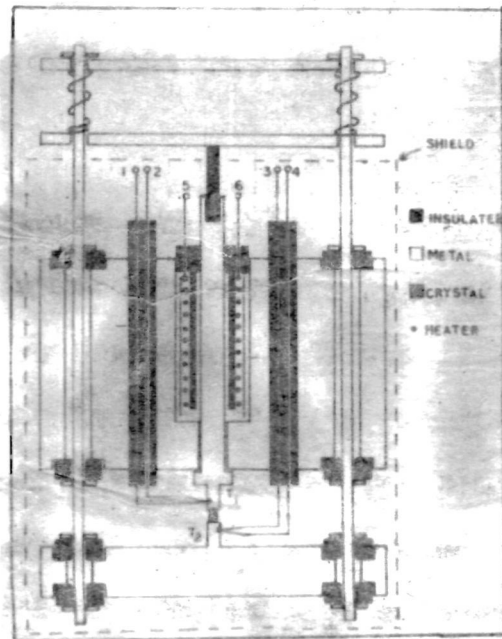is shown in Fig. 8.

FIG.8. CIRCUIT FOR T.E.M.F. MEASUREMENTS.

FIG 9. SAMPLE HOLDER FOR T.E.M.T. MEASUREMENTS.

Because of the high impedance levels at which these amplifiers operate, extreme care was taken by using proper shielding arrangement to reduce the noise pick-up. Since changes in capacitance between input wiring and other objects causes extraneous voltages at the input, the wiring was made as rigid and as short as possible and spaced as far as possible from other objects. A good insulation of the components and wiring associated with the input signal terminals was obtained by using teflon standoffs.

By shorting the input terminals the zero off-set was made by varying the potentiometer R_1, and then the signal to be measured was fed to the input terminal through a coaxial connector. Gain of the BR 3431 J/K was adjusted to 100 and the output voltage was measured on the D.C. microvoltmeter.

The sample-holder used for the measurements of t.e.m.f. is shown in Fig. 9. Two chromel-alumel thermo-couples were fused to the electrodes and were used to measure the temperatures at both ends of the sample. T.e.m.f. was measured across terminals 1 and 2. Since the In-Ga contacts were deposited on the two plane faces of the crystal, graphite spacers were used to protect the deterioration of the contacts. The temperature of the sample was varied by using a conventional tube type
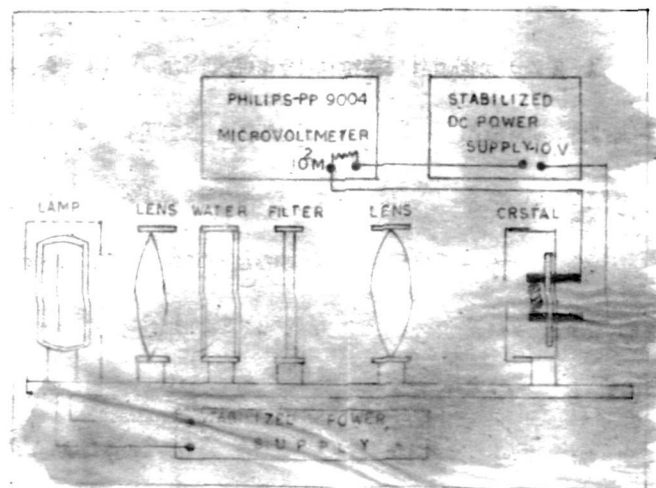
PHILIPS-PP 9004
MICROVOLTMETER

STABILIZED
DC POWER
SUPPLY-10 V

LAMP LENS WATER FILTER LENS CRSTAL

STABILIZER POWER SUPPLY

FIG.6. APPARATUS FOR SPECTRAL RESPONSE MEASUREMENTS

resistance heated furnace and the temperature difference
of the order of 10° was introduced by energizing the
microheater situated at one end. The thermoelectric power
is the ratio thermoelectric voltage and temperature
difference and presented in units of $\mu V/deg$. All the
measurements were made in vacuum.

2.9 SPECTRAL RESPONSE MEASUREMENTS

For spectral response measurements the apparatus
shown in Fig. 10 was used. A tungsten lamp (300 watt)
was used as the source of light. Temperature of the
tungsten filament was measured by optical pyrometer and
its emissivity values for various wavelengths were obtained
from "Hand Book of Physics and Chemistry". Next to the
lamp was placed a convex lens and its distance from the
lamp was so adjusted that a parallel beam of light was
obtained. The heat radiations were absorbed in the distil-
led water contained in a perspex flat (wall) box. To
obtain radiation of different wavelengths, optical filters
of known transmittance made by Carl Zeiss, Germany
in the steps 35ᴼ mμ, 375 mμ, 400 mμ......... to 1000 mμ
were used by placing one at a time and next to the water
trap. This filtered monochromatic radiation was then
condensed by using a convex lens at L_2 and was allowed to
fall on the crystal placed at the focus of L_2. Photocurrent

for each wavelength was measured as described earlier in
the electrical conductivity measurements with the help of
the PP9004 D.C. microvoltmeter and a stabilized D.C. power
supply of 10 volts. The photocurrent was then normalized
by multiplying by the factor T_{600}/T_x where T_{600} is the
transmittance of the filter of wavelength 600 mμ and T_x
is the transmittance of the filters of other wavelengths.
Since the emissivity of the tungsten lamp varies linearly
but negligibly small from its value 0.46 for 350 mμ to its
value 0.42 for 1000 mμ at 1600°C, its correction in the
photocurrent was neglected.

Sample holder for holding the crystal (the same
which was used in electrical conductivity measurements)
was enclosed in a metallic box which shielded the crystal
from other light sources and the electrical noise sources.

In-Ga contacts were made as described earlier.
However, the contacts which were annealed at 350°C in
vacuum could only produce photoconductivity. This
indicates that the In-Ga contacts become ohmic only after
annealing at 350°C.

*****

CHAPTER - 3 : RESULTS AND DISCUSSION
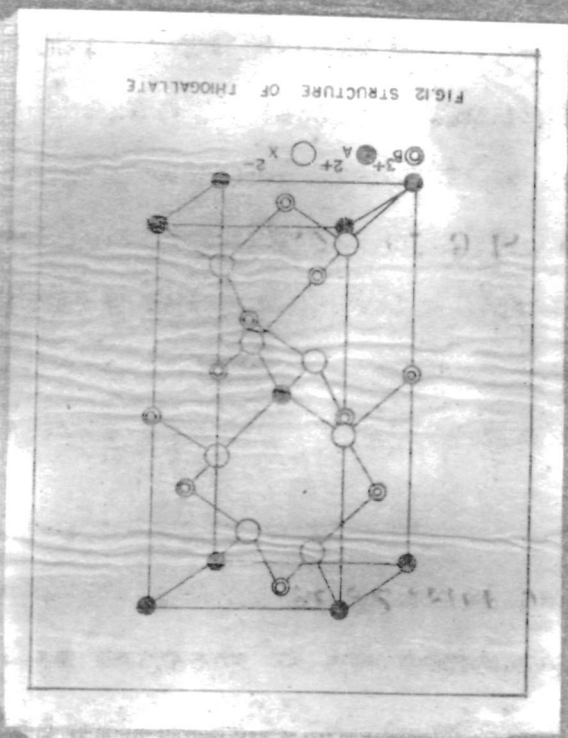
R E S U L T S   A N D   D I S C U S S I O N

3.1 RESULTS OF X-RAY DIFFRACTION

Polycrystalline Materials Data

As indicated earlier the polycrystalline samples of compounds $CdGa_2S_4$, $CdGa_2S_3Se$, $CdGa_2S_2Se_2$, $CdGa_2S_1Se_3$ and $CdGa_2Se_4$ were analysed by the Debye-Scherrer X-ray diffraction method. The Debye-Scherrer patterns of these compounds are presented in Fig. 11.

The compound $CdGa_2S_4$ was first prepared by Hahn et al.[8] and found to have a tetragonal structure very similar to chalcopyrite ($I\overline{4}2d$) and a space group $I\overline{4}$ (or S_4^2). The typical structure of this compound which was named as thiogallate may formally be derived from the chalcopyrite structure by omitting the copper atoms at 1/4 and 3/4 heights. The atomic positions for $CdGa_2S_4$ then may be written with origin at $\overline{4}$, as
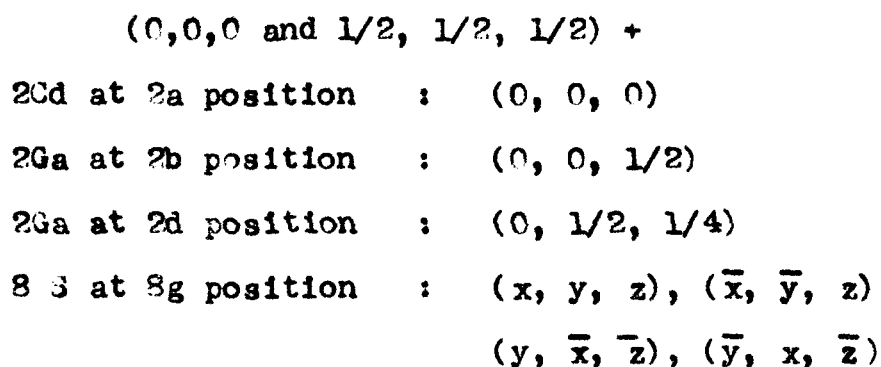
$$(0,0,0 \text{ and } 1/2, 1/2, 1/2) +$$

2Cd at 2a position   : $(0, 0, 0)$

2Ga at 2b position   : $(0, 0, 1/2)$

2Ga at 2d position   : $(0, 1/2, 1/4)$

8 S at 8g position   : $(x, y, z), (\overline{x}, \overline{y}, z)$

$(y, \overline{x}, \overline{z}), (\overline{y}, x, \overline{z})$

Fig. 11-(e) $CdGa_2Se_4$.

Fig. 11-(d) $CdGa_{2.5}Se_3$

Fig. 11-(c) $CdGa_{2.5}Se_3$

Fig. 11-(b) $CdGa_{2.5}Se_4$

Fig. 11-(a) $CdGa_{2.5}Se_3$
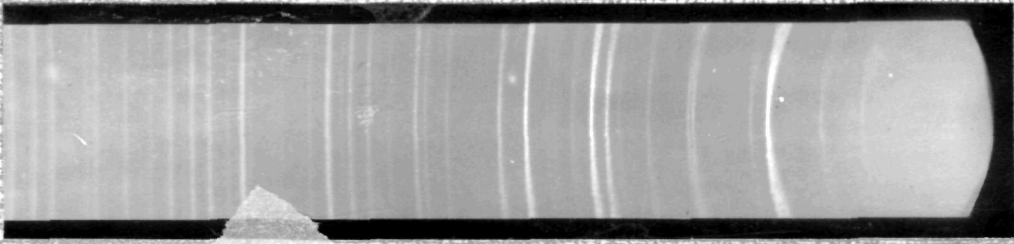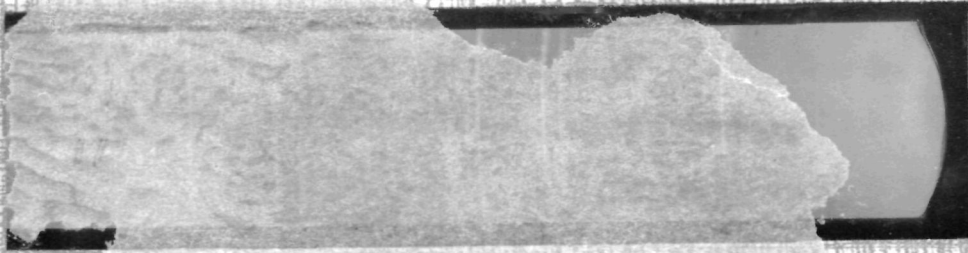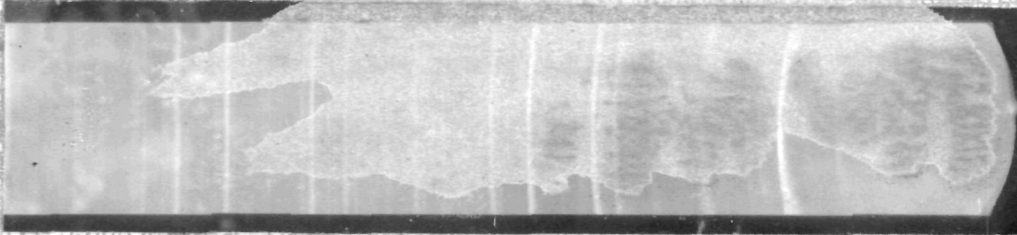
The general condition limiting possible reflections is
$h + k + l = 2n$. The ideal values of x, y and z for the
chalcopyrite structure are 1/4, 1/4 and 1/8 respectively.
For thiogallate ($CdGa_2S_4$) structure the values of x, y
and z were duduced by Hahn et al.[3] as 0.26, 0.27 and
0.14 respectively. The tetragonal unit cell of $CdGa_2S_4$,
thiogallate structure, is illustrated in Fig. 12. The
unit cell contains two molecules of $CdGa_2S_4$.

Though the lattice parameters were obtained for
$CdGa_2Se_4$ by Hahn et al.[3], the detail analysis for x, y
and z parameters for selenium was not made. We have
therefore presented the same in the following section.

The Debye-Scherrer patterns of the compounds
$CdGa_2S_3Se$, $CdGa_2S_2Se_2$, $CdGa_2S_1Se_3$ and $CdGa_2Se_4$ show a
marked resemblance of the structure of the solid solutions
with those of the end members. The composition $CdGa_2S_3Se$
displays a pattern isomorphous with that of $CdGa_2S_4$ whereas
the patterns of $CdGa_2S_2Se_2$ and $CdGa_2S_1Se_3$ are isomorphous
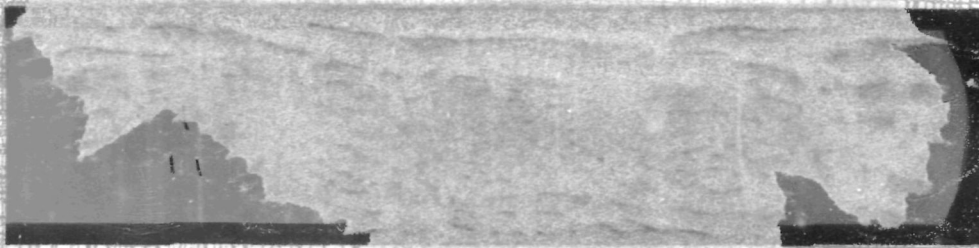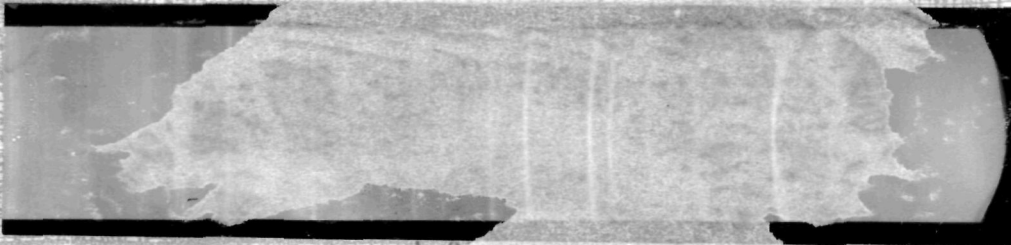with that of $CdGa_2Se_4$. The d-values for these compounds
as calculated from the measurements of the X-ray diffraction
patterns are set out in the Tables 2,3,4,5 and 6. In each
pattern the reflection intensities were estimated visually
as VS, S, MS, M, MW, W, VW, VVW etc. In case of $CdGa_2Se_4$,
the intensity measurements were made on LIRLPHO-2 (Carl
Zeiss) photomicrograph recorder.

TABLE - 2

POLYCRYSTALLINE DIFFRACTION DATA ON $CdGa_2S_4$

hkl	$I_{obs.}$	$d_{(6)}(\overset{o}{A})$	$1/d^2_{obs.}$	$1/d^2_{cal.}$
002	VwB	5.0348	0.0394	0.0337
101	MW	4.3701	0.0422	0.0497
110	MW	3.9104	0.0654	0.0650
112	VS	3.1036	0.1038	0.1036
103	MW	2.8859	0.1201	0.1196
200	MW	2.7675	0.1305	0.1300
004	VW	2.5432	0.1546	0.1547
202	S	2.4364	0.1645	0.1687
211	S	2.4086	0.1724	0.1720
114	MW	2.1290	0.2206	0.2198
213	W	2.0010	0.2498	0.2495
220	M	1.9624	0.2597	0.2598
105	VW	1.9064	0.2752	0.2741
204	S	1.8746	0.2845	0.2847
222	VwB	1.8253	0.3001	0.2986
310	W	1.7552	0.3246	0.3250
006	VW	1.6931	0.3489	0.3481

TABLE - 2 (CONTINUED)

hkl	$I_{obs.}$	d_{obs} (Å)	$1/d^2_{obs.}$	$1/d^2_{cal.}$
312	VS	1.6609	0.3625	0.3641
303	VVW	1.6289	0.3768	0.3778
215	VW	1.5734	0.4039	0.4041
116	M	1.5575	0.4123	0.4130
321	VW	1.5217	0.4320	0.4317
206	W	1.4467	0.4779	0.4783
323	VW	1.4018	0.5088	0.5087
400	M	1.3893	0.5181	0.5198

VS   -   very strong

S   -   strong

MS   -   medium strong

M   -   medium

MW   -   medium weak

W   -   weak

VW   -   very weak

VVW   -   very very weak

B   -   broad

TABLE - 3

POLYCRYSTALLINE DIFFRACTION DATA ON CdGa$_2$S$_3$Se

hkl	$I_{obs.}$	$d_{obs}(\overset{o}{A})$	$1/d^2_{obs.}$	$1/d^2_{cal.}$
002	VWB	5.0519	0.03918	0.0379
101	W	4.8385	0.04271	0.0416
110	MW	3.9172	0.06520	0.0643
112	VS	3.1120	0.10330	0.1022
103	MW	2.9005	0.11890	0.1174
200	VW	2.7809	0.12930	0.1286
004	VVWB	2.5488	0.15390	0.1516
202	MSB	2.4428	0.16760	0.1665
211	MS	2.4161	0.17130	0.1702
114	M	2.1493	0.21650	0.2159
213	W	2.0145	0.24640	0.2460
220	S	1.9746	0.25650	0.2572
105	VVW	1.9286	0.26890	0.2690
204	VS	1.8900	0.27990	0.2802
222	VVW	1.8356	0.29690	0.2951
310	VVW	1.7634	0.32160	0.3215
006	VVW	1.7131	0.34080	0.3411

TABLE - 3 (CONTINUED)

hkl	I_{obs}.	d_{obs} (Å)	$1/d_{obs}^2$.	$1/d_{cal}^2$.
312	VS	1.6603	0.36290	0.3594
303	VVW	1.6466	0.36890	0.3746
215	VVW	1.5933	0.39410	0.3976
116	MS	1.5724	0.40450	0.4054
321	VW	1.5326	0.42580	0.4274
206	W	1.4662	0.46530	0.4697
323	W	1.4120	0.50160	0.5032
400	M	1.3981	0.51170	0.5144

VS	-	very strong
S	-	strong
MS	-	medium strong
M	-	medium
MW	-	medium weak
W	-	weak
VW	-	very weak
VVW	-	very very weak
B	-	broad

TABLE - 4

POLYCRYSTALLINE DIFFRACTION DATA ON $CdGa_2S_2Se_2$

hkl	$I_{obs.}$	$d_{obs.}$ Å	$1/d^2_{obs.}$	$1/d^2_{cal.}$
002	VVVw	5.0348	0.03944	0.0372
101	W	4.8543	0.04244	0.04107
110	W	3.9172	0.06540	0.0635
112	Vs	3.1335	0.10180	0.1008
103	W	2.9246	0.11690	0.1155
200	-	-	-	-
004	-	-	-	-
202	MS	2.4609	0.16510	0.1643
211	MS	2.4325	0.16900	0.1682
114	MW	2.1651	0.21330	0.2122
213	W	2.0307	0.24260	0.2426
220	S	1.9827	0.25440	0.2542
105	VVW	1.9467	0.36400	0.2644
204	Vs	1.9072	0.27500	0.2758
222	VW	1.8461	0.29350	0.2914
310	VVW	1.7768	0.31700	0.3177
006	VVW	1.7299	0.33410	0.3349

TABLE - 4 (CONTINUED)

hkl	$I_{obs.}$	$d_{obs.}$ Å	$1/d^2_{obs.}$	$1/d^2_{cal.}$
312	VS	1.6322	0.35340	0.3549
303	-	-	-	-
215	VVW	1.5988	0.39150	0.3913
116	S	1.5878	0.39700	0.3984
321	VVW	1.5414	0.42090	0.4224
314	W	1.4691	0.46340	0.4664
206	-	-	-	-
323	W	1.4223	0.49430	0.4968
400	MW	1.4078	0.50440	0.5084

VS	-	very strong
S	-	strong
MS	-	medium strong
M	-	medium
MW	-	medium weak
W	-	weak
VW	-	very weak
VVW	-	very very weak
B	-	broad

TABLE - 5

POLYCRYSTALLINE DIFFRACTION DATA ON $CdGa_2Se_3$

hkl	$I_{obs.}$	$d_{obs.}$ Å	$1/d^2_{obs.}$	$1/d^2_{Cal}$
002	VwB	5.1633	0.03743	0.0361
101	W	4.9238	0.04124	0.0401
110	W	3.9691	0.06350	0.0622
112	VS	3.1750	0.09920	0.0983
103	W	2.9760	0.11290	0.1123
200	--	-	-	-
004	--	-	-	-
202	MS	2.4872	0.16170	0.1605
211	MS	2.4583	0.16550	0.1645
114	MW	2.2025	0.20610	0.2065
213	W	2.0544	0.23690	0.2366
220	S	2.0035	0.24920	0.2488
105	--	-	-	-
204	VS	1.9363	0.26670	0.2687
222	VW	1.8595	0.28930	0.2849
310	VVW	1.7937	0.31080	0.3111
006	VVW	1.7634	0.32150	0.3247
312	VS	1.7007	0.34570	0.3472

TABLE - 5 (CONTINUED)

hkl	$I_{obs.}$	$d_{obs.}$ Å	$1/d^2_{obs.}$	$1/d^2_{cal.}$
303	VVW	1.6659	0.36030	0.3611
215	-	-	-	-
116	S	1.6184	0.38190	0.3869
321	VVW	1.5608	0.41050	0.4133
206	W	1.4882	0.45150	0.4491
323	W	1.4403	0.48210	0.4855
400	MW	1.4215	0.49490	0.4976

VS	-	very strong
S	-	strong
MS	-	medium strong
M	-	medium
MW	-	medium weak
W	-	weak
VW	-	very weak
VVW	-	very very weak
B	-	broad

TABLE - 6

POLYCRYSTALLINE DIFFRACTION DATA ON $CdGa_2Se_4$

hkl	$I_{obs.}$	$d_{obs.}$ Å	$1/d^2_{obs.}$	$1/d^2_{cal.}$
002	-	-	-	0.0347
101	M	5.0633	0.03901	0.0390
110	MW	4.0513	0.06094	0.0607
112	VS	3.2360	0.09550	0.0954
103	W	3.0354	0.10860	0.1084
200	VW	2.8678	0.12160	0.12148
004	-	-	-	0.1387
202	W	2.5297	0.15630	0.1562
211	W	2.4973	0.16040	0.1605
114	W	2.2349	0.20020	0.1994
213	VW	2.0832	0.23050	0.2299
220	MS	2.0256	0.24360	0.24296
105	-	-	-	0.2472
204	S	1.9600	0.26030	0.2602
222	VW	1.8312	0.28260	0.2776
310	VW	1.8097	0.30520	0.3037
006	VW	1.7931	0.31110	0.3121

TABLE - 6 (CONTINUED)

hkl	$I_{obs.}$	$d_{obs.}$ Å	$1/d^2_{obs.}$	$1/d^2$
312	S	1.7190	0.33840	0.3384
303	-	-	-	0.3513
215	-	-	-	0.3686
116	M	1.6391	0.37230	0.3728
321	VW	1.5764	0.40260	0.3980
206	-	-	-	0.4335
314	W	1.5038	0.44210	0.4424
323	W	1.4539	0.47300	0.4728
400	M	1.4367	0.48440	0.4859

VS — very strong
S — strong
MS — medium strong
M — medium
MW — medium weak
W — weak
VW — very weak
VVW — very very weak
B — broad

The various lines were indexed with the help of the standard c/a vs log d chart for tetragonal symmetry. All the three new compositions, $CdGa_2S_3Se$, $CdGa_2S_2Se_2$ and $CdGa_2S_1Se_3$ were found to satisfy the conditions h + k + l = 2n, leading to the space group $I\bar{4}$ as that of the thiogallate structure.

The intensity of the strongest line 204 was taken as 100. The observed intensities relative to line (204) of reflections 002, 004, 105, 206 etc. were found to decrease with increasing selenium content. These reflexions were present with appreciable intensities in case of the compound $CdGa_2S_4$, whereas the intensities decreased with increasing content of selenium in the solid solution and were absent when selenium content was more than 50 mol. %.

The lattice parameters were calculated by using the formula,

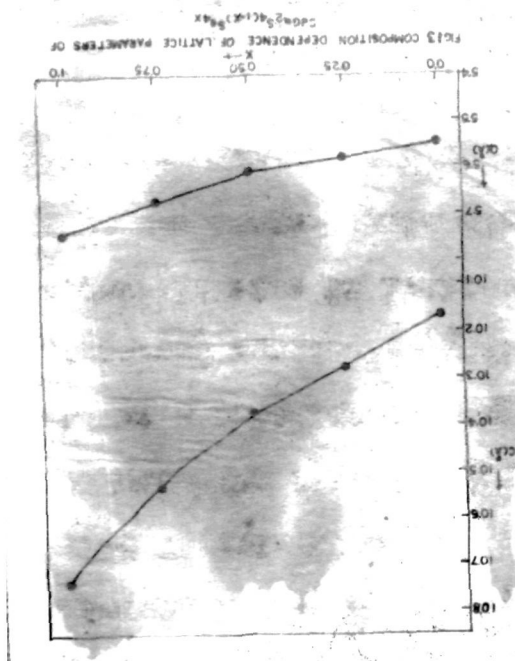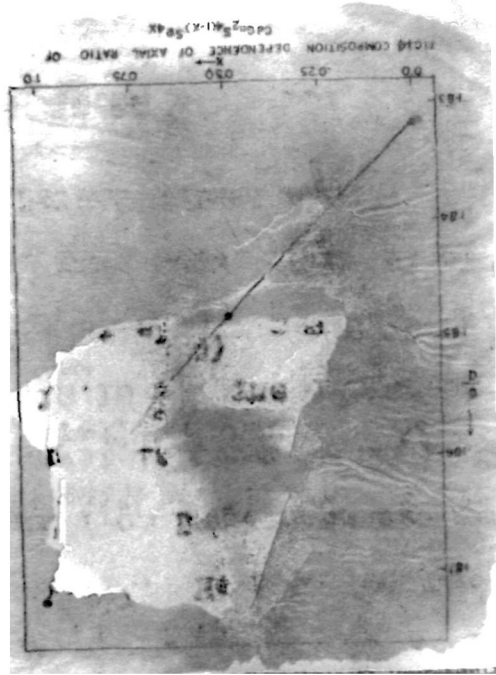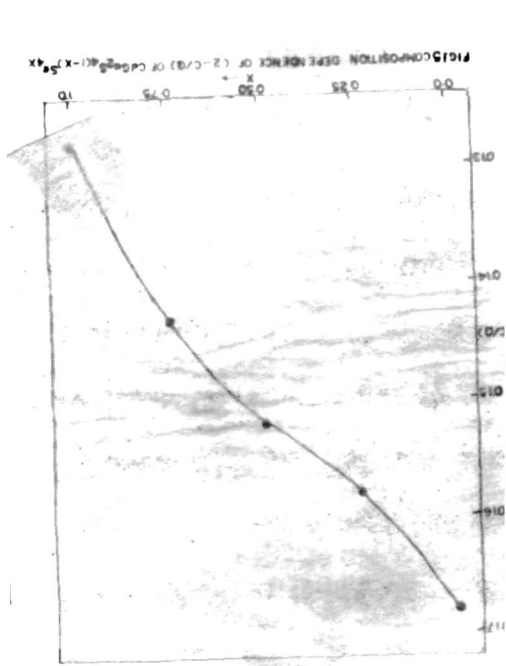$$\frac{1}{d^2} = \frac{h^2 + k^2}{a^2} + \frac{l^2}{c^2}$$

The values of lattice parameters as obtained from polycrystalline data are set out in the Table-7. The dependence of lattice parameters, c/a ratio and the tetragonality factor 2-c/a on composition are plotted in Figs. 13, 14 and 15. The c/a ratio is found to increase

TABLE - 7

CRYSTALLOGRAPHIC DATA OF THE SYSTEM

$$CdGa_2S_{4(1-x)}Se_{4x}$$
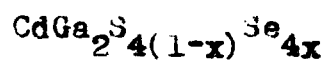
Composition	a ($\overset{o}{A}$)	c ($\overset{o}{A}$)	c/a	2-c/a
$CdGa_2S_4$	5.548	10.170	1.832	0.168
$CdGa_2S_3Se$	5.577	10.275	1.842	0.158
$CdGa_2S_2Se_2$	5.610	10.370	1.848	0.152
$CdGa_2SSe_3$	5.670	10.530	1.857	0.143
$CdGa_2Se_4$	5.738	10.738	1.872	0.128

These various values of lattice parameters reported by different workers indicate a non-stoichiometry of the compound. The lower values indicate the deficiency of the sulphur and the higher values may be thought to come from excess of sulphur.

On the other hand, there is only one report by Hahn et al.[8] on $CdGa_2Se_4$ where the lattice parameters were found to have values

$$a = 5.742 \text{ Å}, \quad c = 10.73 \text{ Å} \quad \text{with} \quad c/a = 1.87.$$

The values of lattice parameters as obtained from poly-crystalline data of the present study are

$$a = 5.738 \text{ Å}, \quad c = 10.738 \text{ Å}, \quad c/a = 1.872$$

which are in close agreement with those of the Hahn et al.[8]

Our X-ray powder diffraction measurements of $CdGa_2Se_4$ revealed absence of reflections (002), (004), (105), (206) etc. Such absence of reflections may be correlated to two factors viz. (1) increase in mass absorption coefficient in going from sulphur to selenium and (2) change in values of parameters x, y and z from sulphur to selenium (Hahn et al. deduced the values 0.26, 0.27 and 0.14 for sulphur). Assuming these values of x, y, and z for selenium and changing mass absorption

coefficient alone did not give satisfactory explanation for the absence of the reflections. We have therefore calculated the intensities of several reflections by giving a set of new values to x, y and z.

The following procedure was adopted for the calculations. The intensities of the observed reflections were assumed to be proportional to the height of the peaks in the photomicrograph and then assuming the intensity of 204 reflection to be 100, apparent intensity ($I_{app(hkl)}$) was obtained by using equation (1)

$$I_{app(hkl)} = \frac{\text{Peak height (hkl)}}{\text{Peak height (204)}} \times 100 \quad \ldots \ldots \quad (1)$$

These I_{app} values were then converted to true intensities by multiplying by the absorption correction $A^*(\theta)$ equation (2)

$$I_{true(hkl)} = \frac{I_{app(hkl)} \times A^*_{(\theta_{hkl})}}{A^*(\theta_{204})} \quad \ldots \ldots \quad (2)$$

Then the squares of the structure factors F^2 were obtained by dividing the I_{true} values by Lorentz, polarization and multiplicity factors as in equation (3)

$$F^2_{true(hkl)} = \frac{I_{true(hkl)}}{L_{hkl}P_{hkl}J_{hkl}} \times \frac{L_{204} P_{204} J_{204}}{} \quad \ldots \ldots \quad (3)$$

These observed squares of the relative structure factors were then compared with those calculated theoretically. Theoretical values were obtained from the equation (4) for space group $(I\bar{4})^{(49)}$

$$F^2_{cal(hkl)} = \frac{(A^2_{hkl} + A^2_{h\bar{k}l} + B^2_{hkl} + B^2_{h\bar{k}l})}{F^2_{cal(204)}} \quad \dots \dots (4)$$

where

$$A = 2f_{Cd} + 2f_{Ga}\left[\cos\pi l + \cos\frac{\pi}{2}(h+k)\cdot\cos\frac{\pi}{2}(h-k)\cos\frac{\pi}{2}l\right]$$

$$+ 8f_{Se}\cos\pi\left[(h-k)x + (h+k)y\right]\cos\pi\left[(h+k)x - (h-k)y\right]$$

$$\cdot \cos(2\pi l z)$$

$$\dots \dots (5)$$

$$B = 2f_{Ga}\left[\sin\frac{(h+k)}{2}\pi \sin\frac{(h-k)}{2}\pi \sin\frac{\pi}{2}l\right] - 8f_{Se}\left[\sin\pi(p)\right.$$

$$\left. \sin\pi(q) \sin(2\pi l z)\right]$$

$$\dots \dots (6)$$

where $p = (h-k)x + (h+k)y$ and $q = (h+k)x - (h-k)y$. f_{Cd}, f_{Ga}, f_{Se} are the scattering powers of Cd, Ga and Se respectively.

$B = 0$ if $h = k = 0$ or $l = 0$.

Since for the reflections 002, 004, 006, 008 etc. the values of A and B depend only on z parameter, the calculations for the absence of 002, 004 etc. indicated that the best value for z = 0.15.

Next for the reflections 200, 400, 110, 220, 600, 310, 800 depend only x and y. The reflections 200, 400, 220, 312, 103 were found to be sensitive to variation in values of x and y. Various values of x and y e.g. 0.200, 0.225, 0.250, 0.275, 0.300 were substituted in equations (5) and (6) for each reflection. The best match was observed for x = y = 0.250 with μR = 4.0 and z = 0.15. The observed and calculated values of F^2 are compared in Table-8. The values of F^2 were normalized further by multiplying by a normalisation factor $\dfrac{\Sigma \mid F^2_{cal} \mid}{\Sigma \mid F^2_{true} \mid}$.

The factor $\quad R \quad = \quad \dfrac{\Sigma \mid F^2_{cal} - F^2_{true,nor.} \mid}{\Sigma \mid F^2_{cal} \mid}$

was found to be 12% when the absent reflections were included. If the absent reflections were omitted, the R reduces to 10%.

The various inter-atomic distances that were calculated for $CdGa_2Se_4$ are :

TABLE - 8

COMPARISON OF CALCULATED AND OBSERVED STRUCTURE FACTORS

FOR CdGa$_2$Se$_4$

hkl	I_{app}	I_{true}	F^2_{true} (Normalized)	F^2_{cal}	$1/d^2_{obs}$ $\overset{\circ}{A}{}^{-2}$	$1/d^2_{cal}$ $\overset{\circ}{A}{}^{-2}$
002	-	-	-	0.6	-	0.0347
101	12	27	3	4	0.0390	0.0390
110	14	28	10	8	0.0609	0.0607
112	97	161	50	54	0.0955	0.0954
103	21	33	11	5	0.1086	0.1084
200	-	-	-	1.7	-	0.1214
004	-	-	-	0.1	-	0.1387
202	25	33	17	20	0.1563	0.1562
211 + 2$\bar{1}$1	15	20	10	7	0.1604	0.1605
114	21	24	17	20	0.2002	0.1994
213 + 2$\bar{1}$3	11	11	8	6	0.2305	0.2299

TABLE - 8 (CONTINUED)

hkl	I_{app}	I_{true}	F^2_{true} (Normalized)	F^2_{cal}	$1/d^2_{obs}$ $\overset{\circ}{A}^{-2}$	$1/d^2_{cal}$ $\overset{\circ}{A}^{-2}$
220	72	75	132	130	0.2436	0.2430
105	-	-	-	2	-	0.2472
204	100	100	96	100	0.2603	0.2602
222	2	2	2	0.1	0.2826	0.2776
310 + 3̄10	12	12	13	10	0.3052	0.3037
006	10	10	47	47	0.3111	0.3121
312 + 3̄12	89	76	100	107	0.3384	0.3384
303	-	-	-	2	-	0.3513
215 + 2̄15	-	-	-	4	-	0.3686
116	20	17	23	16	0.3723	0.3728
321 + 3̄21	8	6	9	5	0.4026	0.3980
206	-	-	-	5	-	0.4335
314 + 3̄14	17	16	29	29	0.4421	0.4424
323 + 3̄23	11	7	13	4	0.4730	0.4728
400	38	25	101	94	0.4844	0.4859

$$Cd\text{-}Se = 2.59 \text{ Å}$$

$$Ga\text{-}Se = 2.59 \text{ Å}$$

$$Ga\text{-}Cd = 4.058 \text{ Å}$$

$$Se\text{-}Se = 4.058 \text{ Å}, \quad 3.93 \text{ Å} \quad \text{and} \quad 4.058 \text{ Å}.$$

Single Crystal Data of $CdGa_2S_4$

The literature shows that the conventional methods[14,16] of growing single crystals of $CdGaS_4$ have failed to give colourless crystals. The yellowish colour of the crystals has been attributed to the non-stoichiometric composition of the crystal. Nitsche et al.[12] obtained colourless single crystals by the method of CTR. They have used hot zone 50° higher than the cold zone (600°). We tried the same conditions, but our trials failed to give colourless crystals when the temperature difference of $50^{\circ}C$ was used. We therefore tried lower gradients and found that difference of $20\text{-}25^{\circ}$ with cold end at 600° gives colourless crystals.

On the other hand, the $CdGa_2Se_4$ crystals were grown by Nitsche et al.[12] and obtained orange-red single crystals with columnar shape using hot zone at $900^{\circ}C$ and cold zone at $700^{\circ}C$. Agaev et al.[24] used higher concentration of iodine (8 mg./cc.) (than that of Nitsche et al. (5 mg./cc.)) and hot zone of $780^{\circ}C$ and cold zone of $680^{\circ}C$. Though bigger crystals were feasible by method of Agaev et al. these crystals are likely to contain high concentration of

iodine as impurity which is known to affect the forbidden gap. Several hot end temperatures differing by 40 to 50°C were tried. Temperatures above 775°C gave very small crystals of poor quality. Big crystals of minimum size 5 x 2 x 1 mm were obtained in the form of triangular prisms with dark brown colours when hot end temperature of 775°C and cold end temperature of 730°C were used.

For the crystal growth of the solid solutions viz. $CdGa_2S_3Se$, $CdGa_2S_2Se_2$ and $CdGa_2S_1Se_3$ the hot end temperatures more than 700, 750 and 775°C respectively did not yield homogeneously coloured crystals. Generally mixed crystals with yellow and red colours were obtained. The hot end temperatures of 675, 725 and 767°C respectively differing by approximately 40°C from cold end yielded homogeneously coloured crystals.

The colour of the crystals of the solid solutions changed with increasing selenium content. $CdGa_2S_3Se_1$ was dark yellow (amber colour) whereas the compositions $CdGa_2S_2Se_2$ and $CdGa_2SSe_3$ were brown and dark brown respectively. The continuous change of colour from colourless for $CdGa_2S_4$ to that of dark brown for $CdGa_2Se_4$ is an indication of the fact that the crystals of single phase solid solutions have been formed.

The shape of the crystals of the solid solutions was of two types. The composition $CdGa_2S_3Se$ crystallized with the shape of a polyhedral crystals as that of $CdGa_2S_4$, whereas the compositions $CdGa_2S_2Se_2$ and $CdGa_2S_1Se_3$ crystallized with triangular prism shape as that of $CdGa_2Se_4$.

For the crystal growth of the solid solutions, increasing temperatures of the hot end were required with the increasing content of selenium. The reason for this may be the lower vapour pressure of selenium iodide than that of sulphur iodide.

The rate of crystal growth was higher for $CdGa_2S_4$ than that of the $CdGa_2Se_4$. The 10 gm. of $CdGa_2S_4$ were transported in 3 days, whereas other compositions required more than 5 to 7 days depending on the selenium concentration. The reason for this is that we have selected temperature differences between hot and cold end approximately $40^\circ C$, and that the vapour pressure of selenium iodide is lower than that of sulphur iodide.

The composition of the crystals was determined by taking their powder X-ray diffraction photographs and measuring their lattice parameters. The plots of lattice parameters (Figs. 13, 14 and 15), as obtained from initial polycrystalline data, vs composition were then compared to obtain the composition. Table-9 gives the comparison of

TABLE - 9

COMPARISON OF LATTICE PARAMETERS OF THE CRUSHED SINGLE CRYSTALS
WITH THOSE OF THE INITIAL POLYCRYSTALLINE MATERIALS

Apparent composition	Initial polycrystalline data			S.C. crushed data		
	a $\overset{o}{A}$	c $\overset{o}{A}$	c/a	a $\overset{o}{A}$	c $\overset{o}{A}$	c/a
$CdGa_2S_4$	5.548	10.170	1.832	5.536	10.16	1.835
$CdGa_2S_3Se$	5.577	10.275	1.842	5.572	10.25	1.840
$CdGa_2S_2Se_2$	5.610	10.370	1.848	5.620	10.38	1.847
$CdGa_2S_1Se_3$	5.670	10.530	1.857	5.682	10.55	1.857
$CdGa_2Se_4$	5.738	10.738	1.872	5.74	10.74	1.872

the lattice parameters obtained from crushed single crystals and initial polycrystalline data. It is rather an approximate method of deducing the composition of the crystals but may be taken as the indicative of the fact that the composition of the crystals is nearly the same as is expected in the chemical formulae viz. $CdGa_2S_4$, $CdGa_2S_3Se$, $CdGa_2S_2Se_2$, $CdGa_2SSe_3$ and $CdGa_2Se_4$.

The chemical analysis was made for the volatile component, mainly selenium, which indicated deficiency of selenium of approximately 1 % by weight. The expected and observed weight percentages of Se in these compositions containing Se and of S in $CdGa_2S_4$ are listed in Table-10.

TABLE - 10

CHEMICAL ANALYSIS OF THE VOLATILE

COMPONENT SELENIUM

Apparent composition	Expected weight per cent of Se/S	Observed weight per cent of Se/S
$CdGa_2S_4$	33.74 of S	33.0
$CdGa_2S_3Se$	18.49 of Se	18.3
$CdGa_2S_2Se_2$	33.32 of Se	33.0
$CdGa_2SSe_3$	45.48 of Se	44.5
$CdGa_2Se_4$	55.63 of Se	54.5

Fig. 17 Laue back-reflection photograph of 112 face
of $CdFa_2S_2Se_2$.

Fig 16. Laue back-reflection photograph of 001 face
of $CdFa_2S_4$.
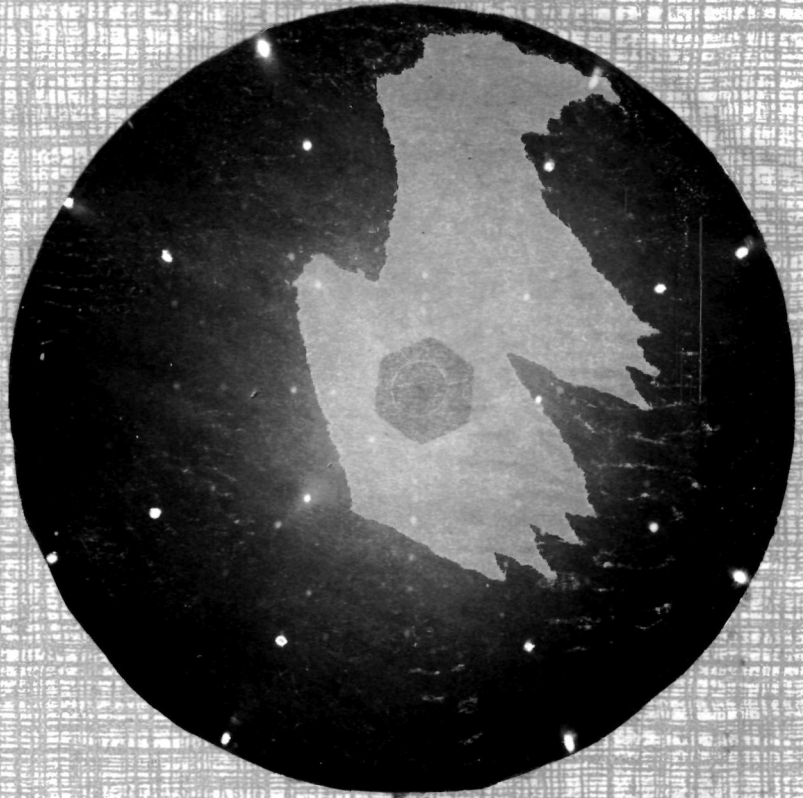
The observed values of selenium content seem to be lower than the one expected. Such deficiency of selenium may be attributed to the following reasons:

(1)   Vapour pressure of selenium is lower than the sulphide.

(2)   Loss of sulphur and selenium in chemical analysis during their reactions with boiling HNO_3.

(3)   Loss of sulphur and selenium in maintaining the dissociation pressure at the crystal growth.

The first two seem to be more likely. The last reason is a little hard to accept as the iodine concentration of 5 mg./cc. in the ampoule maintains a pressure of~10 atmosphere on the material.

Laue-back-reflection photograph from the well developed faces (5 mm x 3 mm) of $CdGa_2S_4$ is presented in Fig. 16. This clearly illustrates a 4-fold symmetry in the distribution of the spots in the photograph. Such a symmetry may be linked with the $\bar{4}$ axis of the crystal space group which must be along the c-axis of the tetragonal unit cell. Hence the well-developed face is the (001) face. This was further confirmed by measuring the rotation X-ray diffraction photograph taken with the rotation axis perpendicular to the face. The value of the axis obtained was 10.21 $\overset{o}{A}$ which is in close agreement with that of 10.16 $\overset{o}{A}$ of the c-axis.

$CdGa_2S_3Se$ gave similar 4-fold symmetry and confirmed that the crystal growth habits of this composition are much similar to that of $CdGa_2S_4$.

The Laue-back-reflection photograph from one of the faces of the triangular prisms of the compound $CdGa_2S_2Se_2$ is presented in the Fig. 17. The arrangement of spots in this photograph seems to have a mirror reflection symmetry on both sides of the vertical line A-A passing through the center of the photograph. The spots on the left hand side have their images on right hand side.

Out of the other two faces of the triangular prism yielded exactly same type of Laue-back-reflection photograph. The third face, however, was not as smooth and optically flat as the first two faces and could not yield a symmetric Laue-back-reflection photograph.

A rotation photograph of the triangular prism with the rotation axis coinciding with the prism edge yielded the value of the unit length along the rotation axis as 8.05 $\overset{o}{A}$ which is in close agreement with the 7.95 $\overset{o}{A}$, obtained by calculations of $\langle 110 \rangle$ unit axial length. This indicates that the triangular prism grows along the $\langle 110 \rangle$ direction. Next the $\langle 110 \rangle$ axis is also a zone axis for the above two faces for which the same Laue-back-reflection photographs were taken.

The angle between the two faces at $\langle 110 \rangle$ direction was
measured by keeping the crystal on a rotating stage of a
spectrometer. This angle was 71°. These planes or faces
were therefore thought to coincide with the (112) planes
as shown in Fig. 18. The calculated angle for $CdGa_2S_2Se_2$
was 74°.

Fig. 18
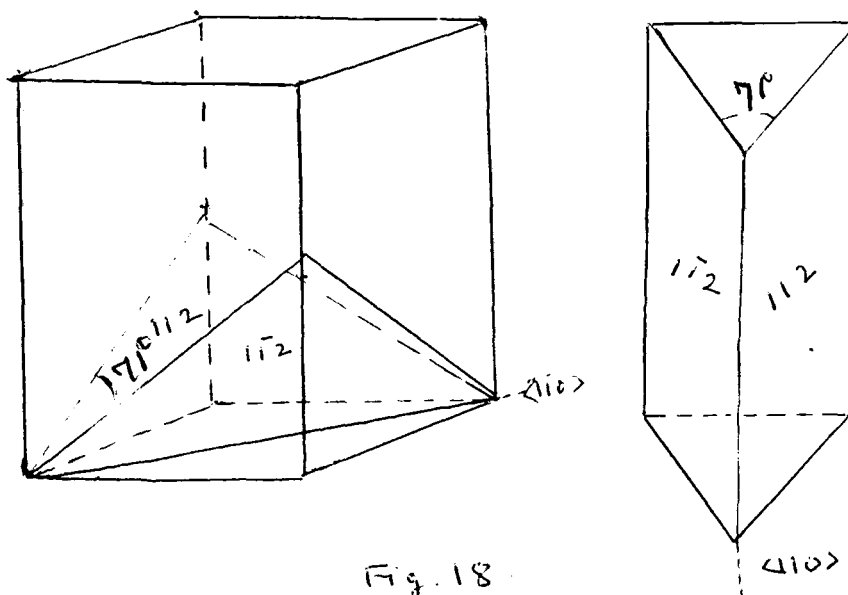
Other compositions $CdGa_2SSe_3$ and $CdGa_2Se_4$ displayed
Laue-back-reflection photographs similar to $CdGa_2S_2Se_2$.
Thus the compositions $CdGa_2S_2Se_2$ and $CdGa_2SSe_3$ may be
assumed to have crystal habits similar to the another
end member $CdGa_2Se_4$.

The properties and crystal growth conditions for
all the compositions are set out in Table-11.

TABLE - 11

THE PROPERTIES AND CRYSTAL GROWTH CONDITIONS FOR VARIOUS
COMPOSITIONS

Composition parameter	$CdGa_2S_4$	$CdGa_2S_3Se$	$CdGa_2S_2Se_2$	$CdGa_2SSe_3$	$CdGa_2Se_4$
Colour	Colourless	Yellow	Brown	Dark brown	Dark brown
Shape	Polyhedral	Polyhedral	Triangular prisms	Triangular prisms	Triangular prisms
Size (mm)^3	5x3x3	5x3x2	7x2x2	10x2x1.5	5x2x1
Hot end $^{\circ}C$	625	675	725	767	775
Cold end $^{\circ}C$	605	630	680	720	730
Iodine mg./cc.	4	4	5	5	5
a $\overset{\circ}{A}$	5.536	5.572	5.620	5.682	5.74
c $\overset{\circ}{A}$	10.16	10.25	10.38	10.55	10.74
c/a	1.835	1.840	1.847	1.857	1.872
Growth direction	001	001	110	110	110

3.2 RESULTS OF ELECTRON DIFFRACTION

Thin Films

In this section results on preparation and structure
of thin films of the compounds $CdGa_2Se_4$ and $CdGa_2S_4$ are
presented. Thin films were prepared by ordinary vacuum
evaporation and flash evaporation. The apparatus used
for the ordinary vacuum evaporation has been discussed in
earlier section. The films were deposited on (100) face
of NaCl single crystals for the purpose of structural
studies, and on thin glass plates or thin quartz plates
for the optical absorption measurements. For both the
compounds the evaporation took place just about $50^{\circ}C$ below
the melting point. In case of $CdGa_2S_4$ occasionally spurt-
ing of the material was observed. $CdGa_2Se_4$ gave deep
brown uniform films whereas $CdGa_2S_4$ films were highly
transparent and colourless or some times with greenish
tint.

Flash evaporation was achieved in the same vacuum
evaporation unit where powder was allowed to fall slowly
on the previously heated tungsten foil. The rate of
powder flow was adjusted by using a vibrator (not shown
in Fig. 6). The temperature of the foil heater was
approximately $900^{\circ}C$ and $1000^{\circ}C$ for $CdGa_2Se_4$ and $CdGa_2S_4$

respectively. $CdGa_2S_4$ gave transparent and colourless
with bluish tint thin films whereas $CdGa_2Se_4$ films were
brown.

Thus it may be seen that the colour appearance of
the thin films of both the compounds is the same as that
in the bulk or single crystal form.

Structure of $CdGa_2Se_4$ Thin Films

The deposits made on substrates at room temperature
did not give any distinct electron diffraction patterns.
This shows that the films were either amorphous or had a
fine grain structure. At higher substrate temperature of
$150^{\circ}C$ the deposits were crystalline having a tetragonal
structure with a = 5.73 $\overset{\circ}{A}$, c = 10.745 $\overset{\circ}{A}$ in agreement with
the X-ray results of the bulk discussed in the first
section of this chapter. The d-values as calculated
from the measurements of the electron diffraction pattern
are given in Table-12. The electron diffraction pattern
of $CdGa_2Se_4$ deposited on substrate (100) NaCl at $150^{\circ}C$ is
given in Fig. 19. Table-12 also shows the comparison of
the d-values obtained from electron diffraction by bulk
sample. Some reflections are found to overlap in case
of electron diffraction patterns. Such behaviour is
commonly observed with several other substances.

TABLE - 12

COMPARISON OF THE d-VALUES OBTAINED FROM
ELECTRON DIFFRACTION AND X-RAY DIFFRACTION

hkl	d values bulk $\mathring{A}$	d values thin film $\mathring{A}$	Intensity observed bulk	Intensity observed thin film
112	3.236	3.24	VS	S
200	2.868	2.85	VW	VW
202	2.530	2.585	W	VW
211	2.490		W	
		2.33		VW
114	2.24		VW	
213	2.08	2.110	VW	VW
220	2.025		M	
		1.984		S
204	1.96		S	
310	1.81	1.83	VW	VW
312	1.72	1.70	S	W
116	1.64	1.65	M	VW
314	1.51	1.53	VW	VW
400	1.43	1.41	MW	W
402	1.34	1.345	M	W

Fig.21
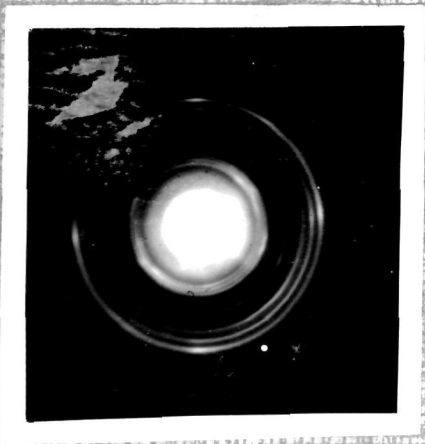
Fig.20
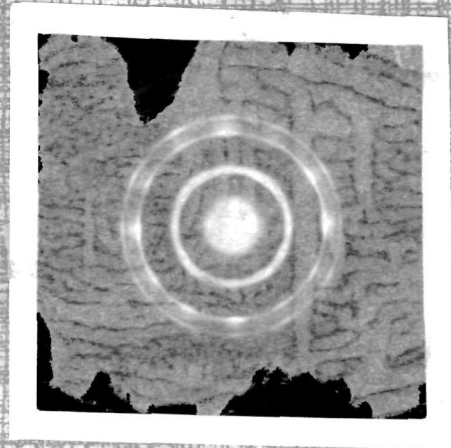
Fig.19(b)
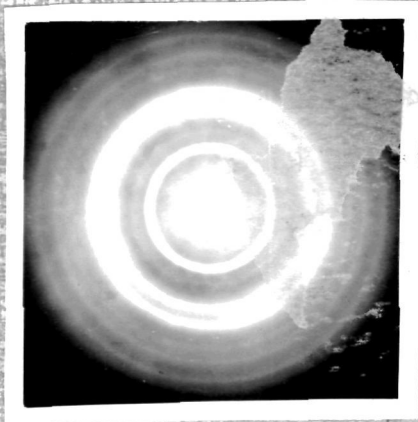
Fig.19(a)
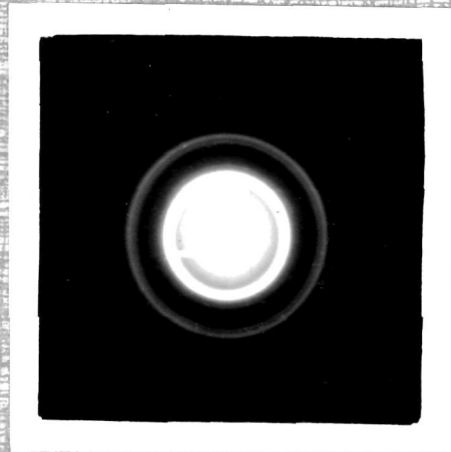
When the substrate temperature was increased to
$200-250^{\circ}C$ a new cubic phase with a = 5.60 $\overset{o}{A}$ was formed
(Fig. 20) and was isomorphous with the sphalerite
structure. Such a behaviour of phase transition has been
observed in the past in case of several chalcogenide
binary and ternary compounds. Chalcopyrite ternary
compounds such as $ZnSnP_2$ have shown phase changes from
tetragonal to cubic depending on the conditions of prepara-
tion even in the bulk form[50].

At still higher substrate temperatures of about
$300-350^{\circ}C$ the deposits gave electron diffraction patterns
indicating that they were mixture of a cubic form
($a_0 = 6.05$ $\overset{o}{A}$) isomorphous with the sphalerite structure
and a hexagonal form (a = 4.3 $\overset{o}{A}$, c = 7.02 $\overset{o}{A}$) isomorphous
with the wurtzite structure. Such a behaviour is likely
to arise from the dissociation of the films at the higher
substrate temperatures. The values of the lattice
parameters of these two phases are close to those of CdSe.
This gave a doubt as to whether it is a CdSe deposit and
not a ternary $CdGa_2Se_4$. However, a qualitative micro-
analysis by using quartz spectrometer showed strong lines
due to the gallium suggesting the presence of a reasonable
amount of gallium in the deposit. Hence the deposit may
still be the ternary compound which has undergone a change
of phase having lattice parameters similar to CdSe. This
is in conformity with the optical absorption data which

showed that absorption edge occurred at wavelength corresponding to the bulk $CdGa_2Se_4$. These results are presented in the next section.

Structure of $CdGa_2S_4$ Thin Films

The deposits made on NaCl (100) substrate at room temperature were amorphous or had a fine grain structure. Deposits made at $300^{\circ}C$ consisted of hexagonal wurtzite phase (a = 4.13 $\overset{\circ}{A}$, c = 6.71 $\overset{\circ}{A}$) and a cubic phase with a = 5.80 $\overset{\circ}{A}$. At substrate temperatures of $400^{\circ}C$, the deposits were mainly hexagonal with a = 4.13 $\overset{\circ}{A}$, c = 6.713 $\overset{\circ}{A}$, resembling CdS. Such a result may not rule out the possibility of dissociation of the compound or thin films at $400^{\circ}C$. A quantitative spectral analysis with the help of quartz spectrometer was made which showed presence of a reasonable amount of gallium in the thin film. Since the electron diffraction photograph (Fig. 21) did not show any phase corresponding to Ga_2S_3 or other gallium sulphide, the deposits may be assumed to undergo a possible phase transition from tetragonal to hexagonal. (In case of $CdGa_2S_4$, when 50% of the gallium was replaced by indium, a hexagonal phase was observed[51] in the bulk.) This is in conformity with the optical absorption data which showed the absorption edge occurred at the wavelength corresponding to the bulk $CdGa_2S_4$. These results are presented in the next section.

3.3 RESULTS OF OPTICAL ABSORPTION

Single Crystal Samples

As indicated in the historical introduction a considerable variation has been observed in reported values of band gaps of $CdGa_2S_4$ and $CdGa_2Se_4$. Such a variation has been attributed to the non-stoichiometric compositions of the crystals. It is also known from the literature that the band gap varies with the direction in crystals along which the absorption or reflection spectrum is studied. However, previous workers have not identified the faces for which they studied optical absorption or reflection spectrum. This may be an additional reason for the observed scatter in the values of energy band gaps of these two compounds. In our present investigation, we have identified, by the Laue-back-reflection photograph, the faces for which we have studied the optical absorption. The compositions $CdGa_2S_4$ and $CdGa_2S_3Se$ gave polyhedral crystals with the biggest face parallel to (001), whereas $CdGa_2S_2Se_2$, $CdGa_2SSe_3$ and $CdGa_2Se_4$ gave triangular prisms with edge $\langle 110 \rangle$ and a face parallel to (112) plane.

Buen et al.[13] reported for $CdGa_2S_4$ the values of wavelength at which α (optical absorption coefficient)

FIG.23 ONSET OF DIRECT TRANSITIONS IN CdGa$_2$S$_4$

FIG.22 ABSORPTION COEFF. VS PHOTON ENERGY
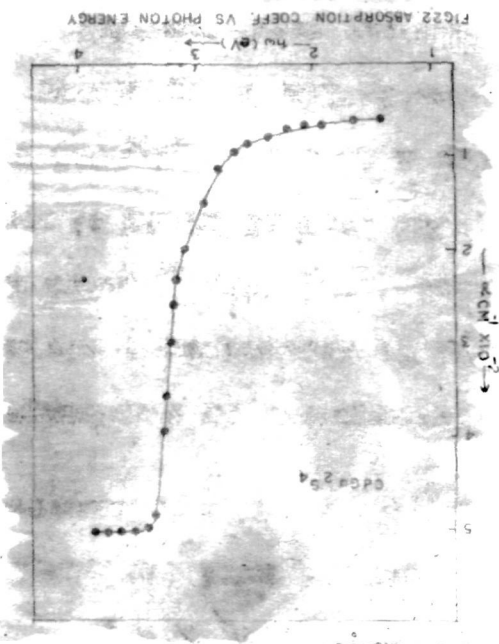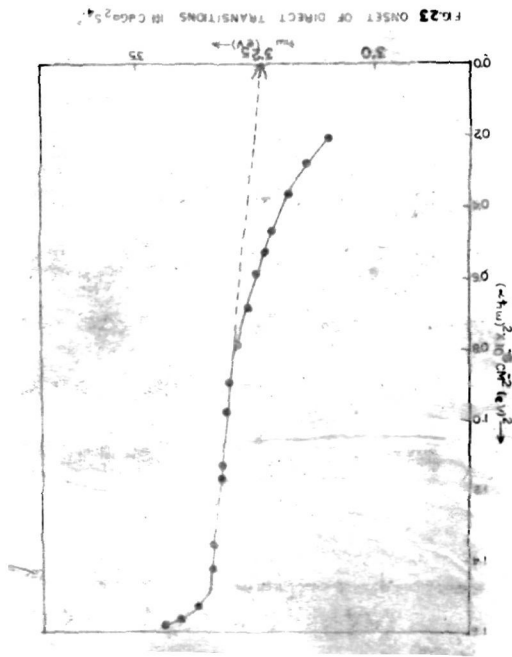
was 500 cm^{-1} as fundamental absorption edge, λ edge = 358 mμ (i.e. 3.45 eV) and did not give the further analysis of the absorption spectrum.

Spectral dependence of the absorption coefficient as calculated from our measurements of transmission through single crystals of CdGa$_2$S$_4$ with (001) face normal to the incident light beam is shown in Fig. 22. The edge of the absorption band of CdGa$_2$S$_4$ occurs at a wavelength 400 mμ which corresponds to energy of 3.1 eV and α = 200 cm^{-1}. Further analysis of this spectrum was made by assuming that the absorption spectrum beyond the absorption edge is due to the direct transitions of electrons between valence band maximum (at $\bar{k}$ = o) and conduction band minimum (at $\bar{k}$ = o). The spectrum then may be theoretically considered to obey the relation,

$$\alpha_d = \frac{\text{constant} \cdot \left[\hbar w - E_g(\text{Dir}) \right]^{1/2}}{\hbar w}$$

which is true only for $\hbar w > E_g(\text{Dir})$ and α_d = 0 when $\hbar w < E_g(\text{Dir})$. The minimum energy gap for the direct transitions then may be obtained by extrapolating the straight line plots of $(\alpha \hbar w)^2$ vs $\hbar w$ to α_d = 0. In case of CdGa$_2$S$_4$ (Fig. 23) the energy gap $E_g(\text{Dir})$ obtained is 3.25 eV.

Further, assuming that the absorption spectrum before
and near the absorption edge is due to the indirect transi-
tions of electrons between valence band maximum at ($\bar{k} = o$)
and conduction band minimum at ($\bar{k} \neq o$), the spectrum was
considered to obey the relation,

$$\alpha_1 = \alpha_{1e} + \alpha_{1a}$$

where α_{1e} is the absorption coefficient due to phonon
emission and α_{1a} is due to the phonon absorption and

$$\alpha_{1e} = \frac{\text{constant} \cdot \left[\hbar w + E_p - E_g(\text{Ind}) \right]^2}{\hbar w}$$

for phonon emission, which is true for $\hbar w > E_g(\text{Ind}) - E_p$
and $\alpha_{1e} = 0$ for $\hbar w < E_g - E_p$.

$$\alpha_{1a} = \frac{\text{constant} \cdot \left[\hbar w - E_p - E_g(\text{Ind}) \right]^2}{\hbar w}$$

for phonon absorption, which is true for $\hbar w > E_g + E_p$
and $\alpha_{1a} = 0$ when $\hbar w < E_g + E_p$.

Since the strong absorption due to the direct transi-
tions overlaps the weak absorption due to the indirect
transitions near the fundamental absorption edge, the
deduction of indirect band gaps needs careful and accurate
analysis of the spectrum. We plotted the $(\alpha_1 \hbar w)^{1/2}$ vs $\hbar w$
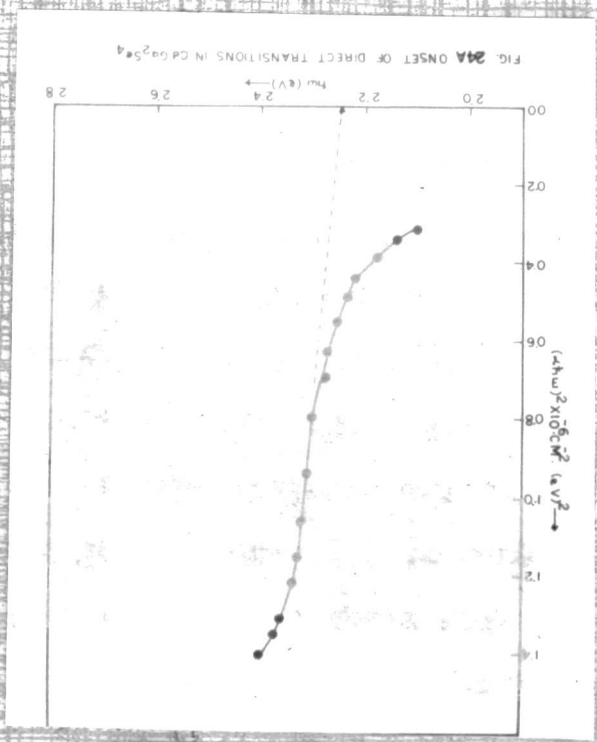for values of α_1 before (the direct transition) 3.25 eV

FIG. 24A ONSET OF DIRECT TRANSITIONS IN Cd Ga₂Se₄

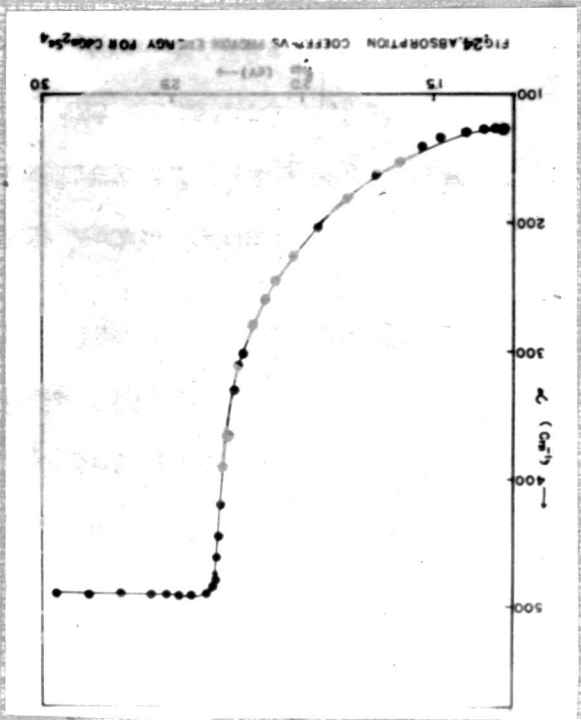FIG. 24 ABSORPTION COEFF. VS. PHOTON ENERGY FOR CdGa₂Se₄

Fig 24A

for $CdGa_2S_4$. However, the plot did not yield convincing support for the presence of indirect transitions which is not in agreement with that of Beun et al.[13]. Our data receives a support from the reflectivity study of $CdGa_2S_4$ in reference (21) that no peaks corresponding to the indirect transition were observed.

On the other hand, Radautsan et al.[30] analysed the absorption spectrum of $CdGa_2Se_4$. They supported data of Beun et al.[13] and obtained $E_g(Dir) = 2.43$ eV and $E_g(Ind) = 2.27$ eV. However the analysis of indirect transition given by Radautsan et al. is rather misleading as energy ranges of the absorption spectrum for the indirect and direct transitions were not considered separately and hence the $\chi^{1/2}$ is most likely to contain absorption values due to direct transitions. Beun et al.[13] have indicated the inadequacy of their data for the support of indirect transitions in this compound also. We have therefore carefully analysed our data of absorption spectrum of $CdGa_2Se_4$ (Fig. 24). The plots of $(\chi_d \hbar w)^2$ vs $\hbar w$ (Fig. 24A) gave $E_g(Dir)$ to be 2.25 eV whereas plots of $(\chi_1 \hbar w)^{1/2}$ vs $\hbar w$ for $\hbar w < 2.25$ eV did not give convincing support for the indirect transitions. This is also in agreement with the reflectivity data in reference (21) as there was no peak due to the indirect transitions.
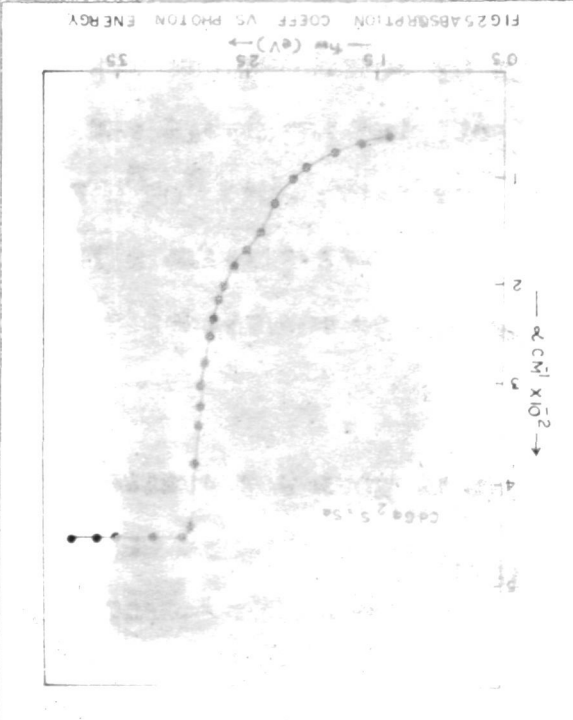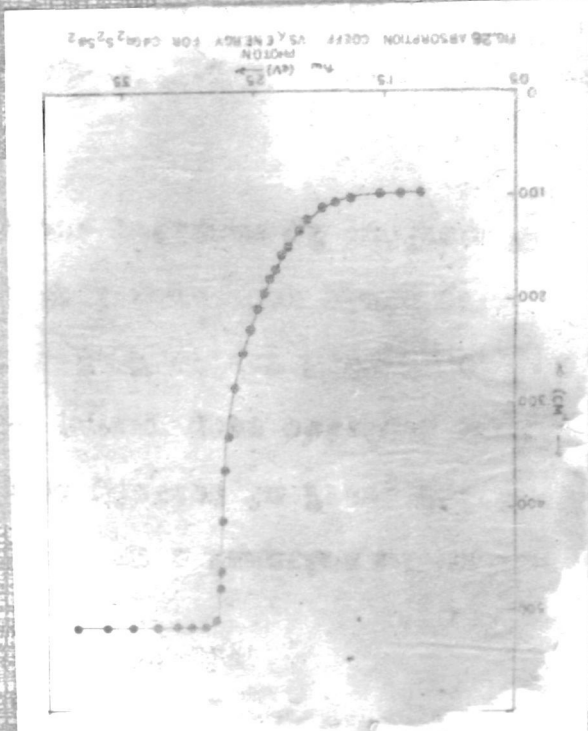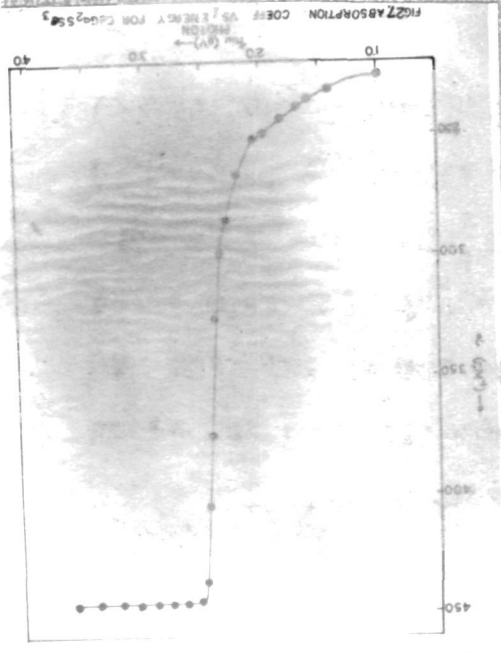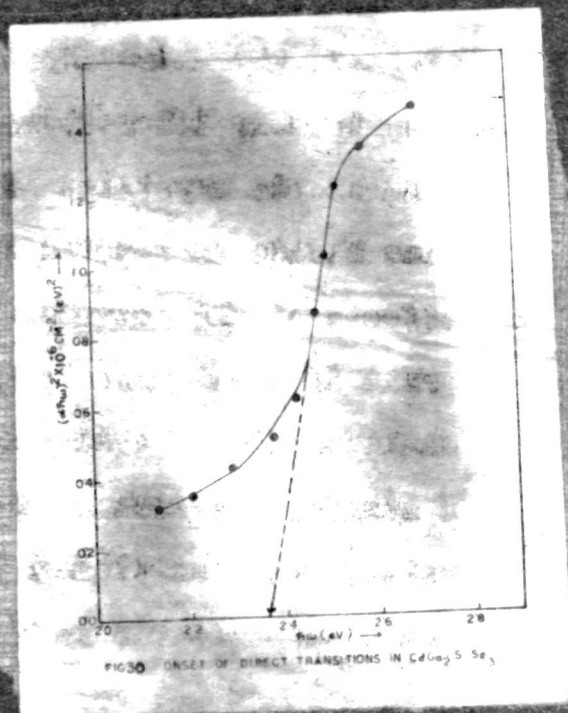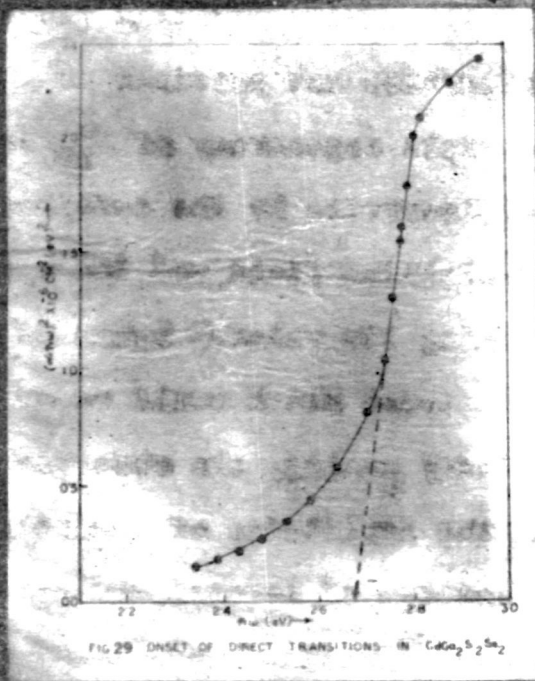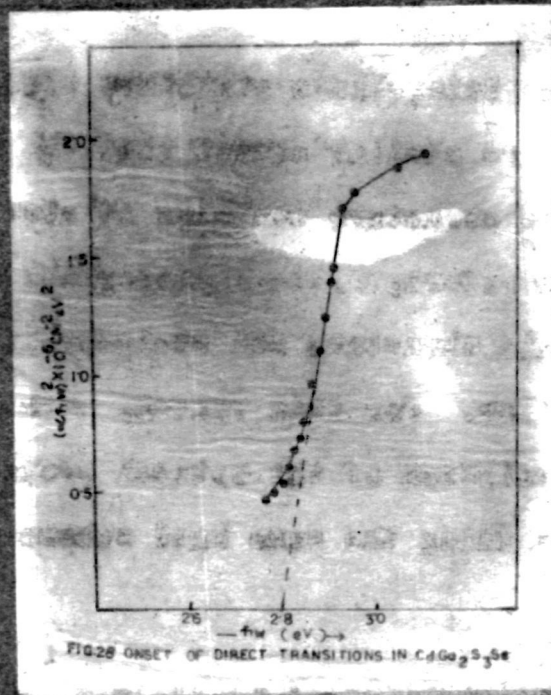
We have, however, observed values of direct band
gaps lower than those of Buen et al.[13] and Radautson
et al.[30]. The reasons for such an observation are not
clear.

The spectral dependence of the absorption coeffi-
cient for the single crystal specimens of $CdGa_2S_3Se$ (for
(001) face), $CdGa_2S_2Se_2$ (for (112) face) and $CdGa_2SSe_3$
(for (112) face) are presented in Figs. 25, 26 and 27.
There is a slow rise in absorption in the long wave region
followed by a steep rise in the short wave region. The
spectra are isomorphous with those of the parent compounds
(Figs. 22,24). The absorption edge was taken at the
start of the steep rise and has values 2.8, 2.65 and
2.45 eV for these compounds respectively.

The variation of $(\alpha_a \hbar w)^2$ as a function of $\hbar w$ for
these new compositions has been plotted in Figs. 28, 29
and 30. The values of direct energy gaps obtained from
these plots are 2.80, 2.67 and 2.37 eV for $CdGa_2S_3Se$,
$CdGa_2S_2Se_2$ and $CdGa_2SSe_3$ respectively. The plots of
$(\alpha_i \hbar w)^{1/2}$ vs $\hbar w$ did not support presence of indirect
transition convincingly.

Our results receive support from the theoretical
analysis of the band structure. Band structure of the
thiogallate semiconductors (i.e. $CdGa_2S_4$ and $CdGa_2Se_4$) is

FIG.28 ONSET OF DIRECT TRANSITIONS IN CdGa₂S₃Se

FIG 29 ONSET OF DIRECT TRANSITIONS IN CdGa₂S₂Se₂

FIG.30 ONSET OF DIRECT TRANSITIONS IN CdGa₂S Se₃

not known. The thiogallate structure ($I\overline{4}$) and the chalco-
pyrite ($I\overline{4}2d$) are similar except that the unit cell in
the thiogallate structure contains 14 atoms and two cation
vacancies. Therefore, optical properties of the substances
with thiogallate structure and chalcopyrite structure
should be similar. For this reason, much of the quali-
tative interpretation of the optical properties may be
obtained by assuming the same band scheme as that of
chalcopyrite.

Semiconductor materials $II-IV-V_2$ crystallizing
with the chalcopyrite structure have physical properties
similar to those of familiar $III-V$ zinc-blende type semi-
conductors. Although two crystal structures are quite
similar, the anisotropy of chalcopyrite crystals gives
rise to many interesting properties not possible in
zinc-blende crystals. The triple degeneracy of Γ_{15} in
zinc blende is removed in chalcopyrite by the combined
effects of the non-cubic crystalline field and the spin-
orbit interaction. By regarding the valence bands of
chalcopyrite as equivalent to those which would occur in
a strained version of its binary analog, the observed
valence band splittings and the amplitudes of the polari-
zation dependences in E.R. spectra of several chalco-
pyrite semiconductors have been explained quantitatively.

The doubling of the unit cell in the z-direction
in chalcopyrite relative to zinc blende causes the

appearance of the pseudo-direct energy band gaps. The
pseudo-direct energy gaps, which are direct gaps in chalco-
pyrite corresponding to indirect gaps in zinc blende,
occur due to the mapping of the zinc blende Brillouin zone
into the smaller chalcopyrite Brillouin zones[52].

The compounds II-III-V_2 may be divided into two
groups[53] : (a) $ZnSnP_2$, $CdSnP_2$, $ZnGeAs_2$, $CdGeAs_2$, $ZnSnAs_2$,
$CdGeP_2$ and $CdSiAs_2$. (b) $MgSiP_2$, $ZnSiP_2$, $ZnGeP_2$, $ZnSiAs_2$
and $CdSiP_2$. Crystals of the first group of II-IV-V_2
compounds are characterized by direct optical transitions
in the region of the fundamental absorption edge, whereas
crystals belonging to the second group may exhibit indirect
transitions[53].

Though for the second group compounds, the band
structure calculations show two minima, one in the Γ point
(representation Γ_3) and another in the point T (represen-
tation $T_1 + T_2$), they are approximately on the same energy
coordinate. In such a situation, the direct transitions
will overlap with the indirect transitions, and the optical
data would reveal the result only as direct transition.

The compounds $CdGa_2S_4$ and $CdGa_2Se_4$ in the present
study may be assumed to be isoelectronic with $CdGeP_2$ and
$CdGeAs_2$ when compared with the electronic structure of Ga
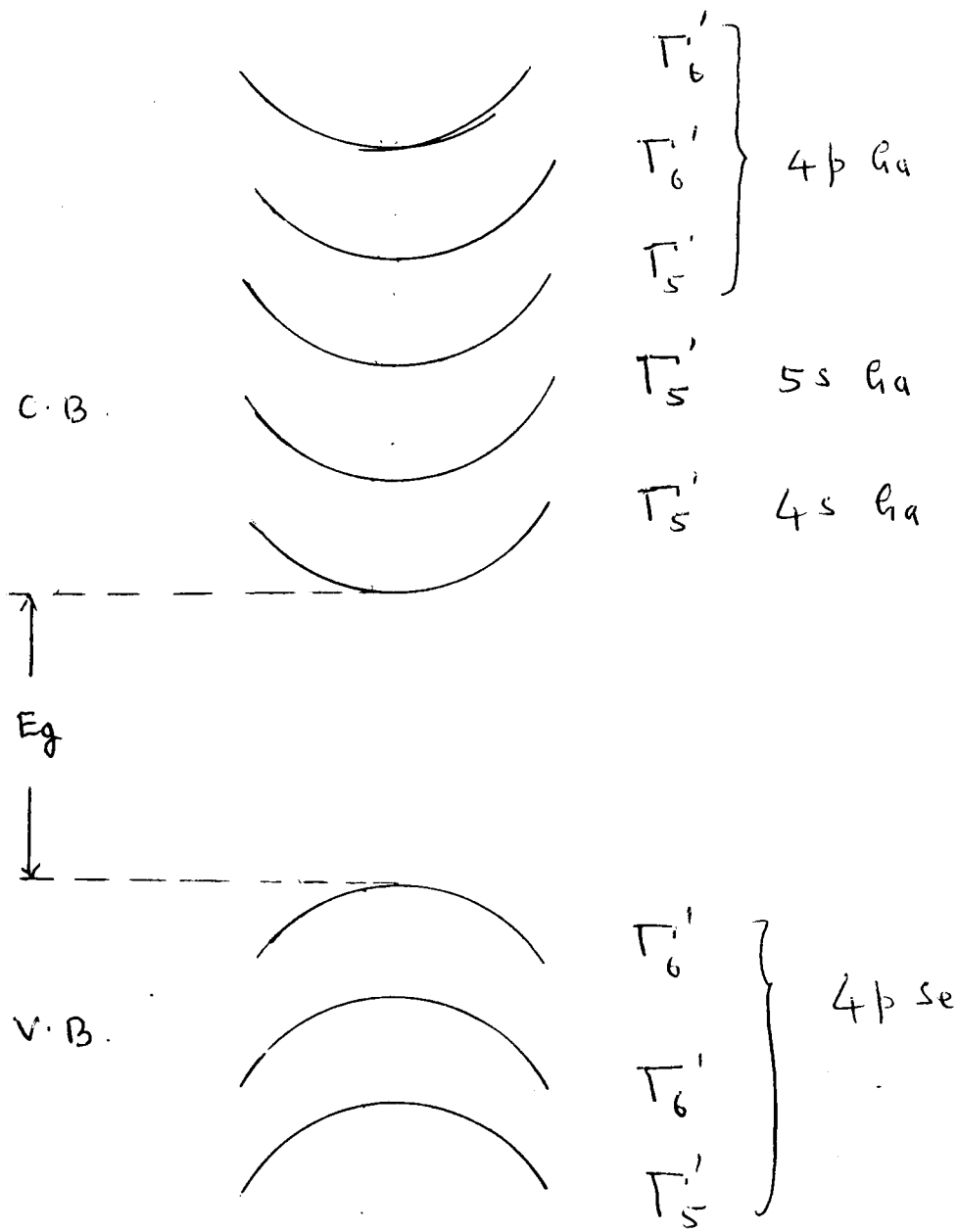and Ge and that of S and P, and of Se and As. Since the

Γ_6'
Γ_6' $\Big\}$ $4p$ Ga
Γ_5'

C·B.

Γ_5' $5s$ Ga

Γ_5' $4s$ Ga

E_g

V·B.

Γ_6' $\Big\}$
Γ_6' $\Big\}$ $4p$ Se
Γ_5'

Fig. 44 A.

Energy Band scheme for $CdGa_2Se_4$ at
point $\overline{K} = 0$

compounds $CdGeP_2$ and $CdGeAs_2$ are characterized by direct
band gap; it may be possible that the compounds under
present study i.e. $CdGa_2S_4$ and $CdGa_2Se_4$ are also direct
band gap materials which is in agreement with our results.

The variation of band gap values obtained from
optical absorption, photoconductivity and thermal varia-
tion of electrical conductivity as a function of composi-
tion is plotted in Fig. 44. (page 108) The plot reveals that the
band gap varies in a rather broad way with composition.
The band gap increases with increasing sulphur contents.
This is also in agreement with the following theoretical
qualitative analysis.

A group theoretical analysis has demonstrated
qualitatively that the band structure of these compounds
is fairly complex[30] (Fig. 44A). The valence sub-bands
are formed from the 4p states of the anions such as
Selenium in case of $CdGa_2Se_4$. The spin-orbit interaction
splits the upper valence band into three sub-bands. The
sub-band $\Gamma_6' = \Gamma_7 + \Gamma_3$ (the irreducible representations
of the $\overline{I4}$ group are labelled in the same way as Heine's
book[54]) originates from the $4p_z$ states in $CdGa_2Se_4$ and
it is split off from the $4p_{x,y}$ states by the crystal field.
The remaining two sub-bands Γ_6' and $\Gamma_5' = \Gamma_5' + \Gamma_6'$ are

formed from the $4p_{x,y}$ states which are split by the spin-orbit interaction. If the crystal field and the spin-orbit interactions are of the same order of magnitude, the splittings become more complex.

An allowance for the presence of two molecules in a unit cell and for the chemical formula of the compound shows that 4p states of the selenium give rise to 24 doubly degenerate sub-bands[30]. Moreover, in the presence of some covalence in the chemical bonding, the 5s shells of Cd as well as the 4s and 4p shells of Ga may contribute to the valence bands.

The conduction subbands are formed from the 4s subband (Γ_5') and the 4p ($2\Gamma_6'$, Γ_5') shells of gallium and from the 5s (Γ_5') shells of Cd. The lowest conduction subband most probably has the Γ_5' symmetry. The symmetry of the uppermost valence subband can be determined without ambiguity from optical measurements because $\Gamma_6' - \Gamma_5'$ direct optical transition is unpolarized, whereas the $\Gamma_5' - \Gamma_5'$ transition (as well as $\Gamma_6' - \Gamma_6'$) is polarized. It may thus be seen that the increase in the direct band gap with increasing sulphur is most likely and agrees with the group theoretical analysis as the conduction subbands remain fixed in all the compositions and the only changes that take place are in valence subbands where the 4p states
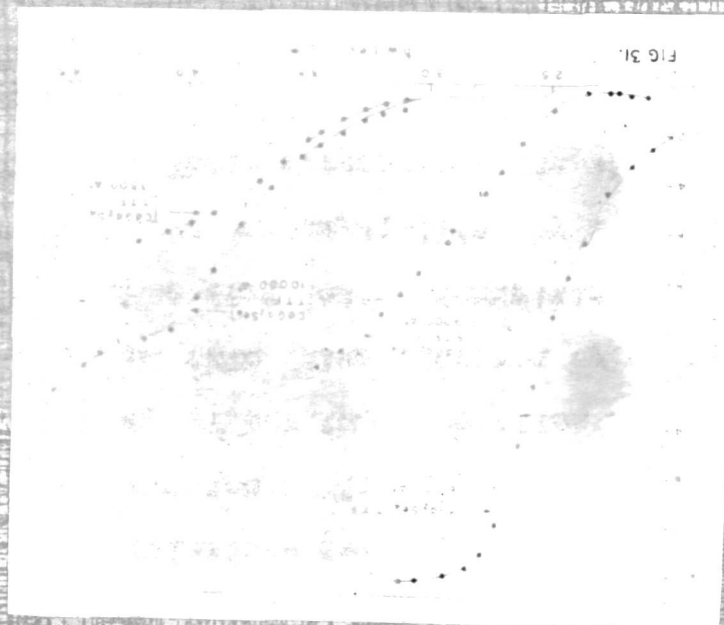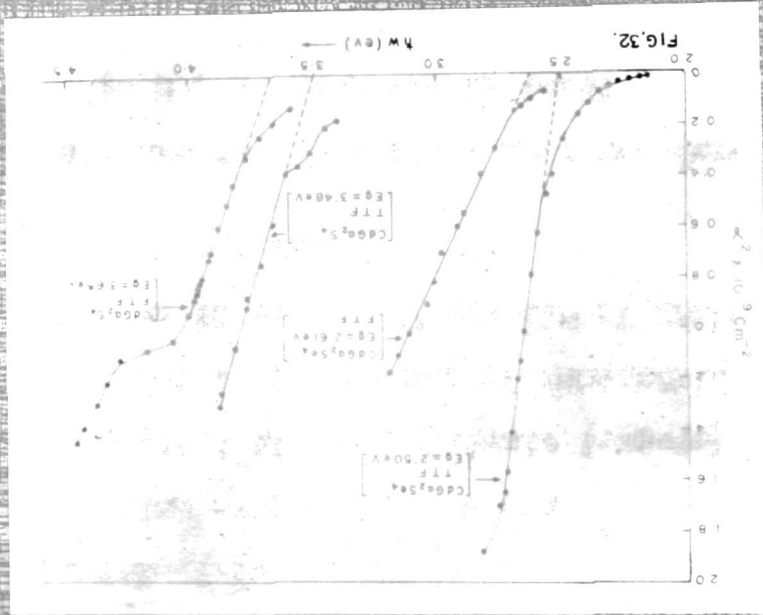
Th 4614

of selenium are replaced by 3p states of sulphur depres-
sing the valence subband lower than that of $CdGa_2Se_4$.

Optical Absorption through
Thin Film Specimens

For semiconductors in the region of the fundamental
absorption edge, the absorption coefficient varies over
several orders of magnitude. When the absorption coeffi-
cient rises to values of the order of 10^6 cm^{-1}, the
penetration depth of radiation is at most a few hundred
Angstroms (i.e. less than 0.1 micron) and the surface
damage that can be tolerated must extend to a depth
considerably less than this. Also the microscopic surface
roughness must be less than the wavelength of the radia-
tion being used, otherwise scattering effects will be
introduced. If crystals are big, one can obtain good
surfaces by cleaving the crystals. When cleavage is not
possible crystals can be ground parallel to some naturally
grown large area surface by mechanical grinding and polish-
ing by hand or machine in several stages using progres-
sively finer abrasives. For absorption measurements, the
minimum thickness obtained by mechanical polishing depends
on the material.

A different approach to sample preparation, parti-
cularly when extremely thin specimens are required, is to
evaporate material, if possible epitaxially, on to a
substrate. Extremely good results may be obtained when a
transparent substrate with the same symmetry and lattice
parameters ($\pm$ 5%) as that of the material to be evaporat-
ed is used. In some cases, however, good polycrystalline
films may be obtained even if these match-conditions are
not fulfilled[55]. This technique has been applied
successfully to various solid solutions of the alkali
halides[56] and in case of single compounds to the lead
salts PbS, PbSe, PbTe[57] and to Bi_2Te_3[58]. Recently
similar method was employed to study the optical absorption
spectrum of polycrystalline films of $CdCr_2S_4$[59].

Crystals of the series of compounds $CdGa_2S_{4(1-x)}Se_{4x}$
were, specially those containing selenium, brittle and it
was not possible to grind them to very thin slices of
thickness less than 100 microns. Again the area of the
ground crystal plates was very small approximately between
1.5 mm x 5 mm to 1.5 mm x 10 mm. Large area and very thin
but polycrystalline films were thought to be advantageous
in studying more precisely the optical properties by trans-
mission measurements. There has been only one note[23]
on thin film preparation of $CdGa_2Se_4$. However, no detail

$\hbar\omega$ (eV)

ε_2, 10^4 cm^{-2}

$\left[\begin{array}{c}\text{CdGa}_2\text{S}_4 \\ \text{TTF} \\ \text{Eg}=3.48\text{eV}\end{array}\right]$

$\left[\begin{array}{c}\text{CdGa}_2\text{S}_4 \\ \text{TTF} \\ \text{Eg}=3.6\text{eV}\end{array}\right]$

$\left[\begin{array}{c}\text{CdGa}_2\text{Se}_4 \\ \text{TTF} \\ \text{Eg}=2.6\text{eV}\end{array}\right]$

$\left[\begin{array}{c}\text{CdGa}_2\text{Se}_4 \\ \text{TTF} \\ \text{Eg}=2.50\text{eV}\end{array}\right]$

FIG 31.

studies such as structure and optical transitions have been made. Next advantage is that the chemical composition in single crystals of these compounds are likely to have small deviations from stoichiometry and that there is also some inclusion of iodine as impurity in the crystal which may affect the absorption edge considerably. On the other hand thin films prepared by vacuum evaporation would be free from iodine impurities and can be made stoichiometric and crystalline by selecting suitable conditions. For these reasons a study of optical absorption through thin films of $CdGa_2Se_4$ and $CdGa_2S_4$ are reported here.

The spectral dependence of log I_0/I as a function of ℏw as obtained from the measurements of transmission through thin films of $CdGa_2S_4$ (on quartz) and $CdGa_2Se_4$ (on glass) deposited at the substrate temperature of $200^\circ C$ is shown in Fig. 31. The values of fundamental absorption edge may be taken to be 2.5 eV and 3.5 eV for $CdGa_2Se_4$ and $CdGa_2Se_4$ respectively.

The electronic transitions near the fundamental absorption edge may be analysed by considering the plots of α^2 vs ℏw for direct transitions (Fig. 32) and $(\alpha ℏw)^{1/2}$ vs ℏw for indirect transitions. Extrapolation of the linear portions of the plots of α^2 vs ℏw to zero absorption gave a value of 2.51 eV for direct transitions in $CdGa_2Se_4$

whereas 3.50 eV in $CdGa_2S_4$. These are the values of
direct band gaps for the thermally evaporated films. The
values of the direct band gaps obtained from the flash
evaporated thin films are 2.64 eV and 3.63 eV respectively.
These values are in reasonable agreement with those 2.55 eV
and 3.58 eV for $CdGa_2Se_4$ and $CdGa_2S_4$ respectively obtained
from reflectivity measurements on single crystals[21] but
are slightly higher than the band gap values obtained
from transmission data on single crystal slices.

The large number of defects present in the evapora-
ted and annealed films will generally tend to decrease the
energy gap[60]. Hence the transmission gap in bulk
material should occur at slightly higher energy than in
the thin films. However, our results are in contradiction
to these expectations. The values of direct band gap
obtained from transmission measurements on single crystals
grown by CTR method vary from 2.0 to 2.4 eV for $CdGa_2Se_4$[13,24,26]
and from 3.2 to 3.45 eV[13,21] for $CdGa_2S_4$. These lower
values possibly indicate the defects in the bulk material
such as the non-stoichiometry of the composition and the
inclusion of the transport agent such as iodine in the
crystals.

The plots of $(\alpha \hbar\omega)^{1/2}$ vs $\hbar\omega$ did not give a convinc-
ing support to the indirect transitions in these thin
films, which is also in agreement with bulk material.
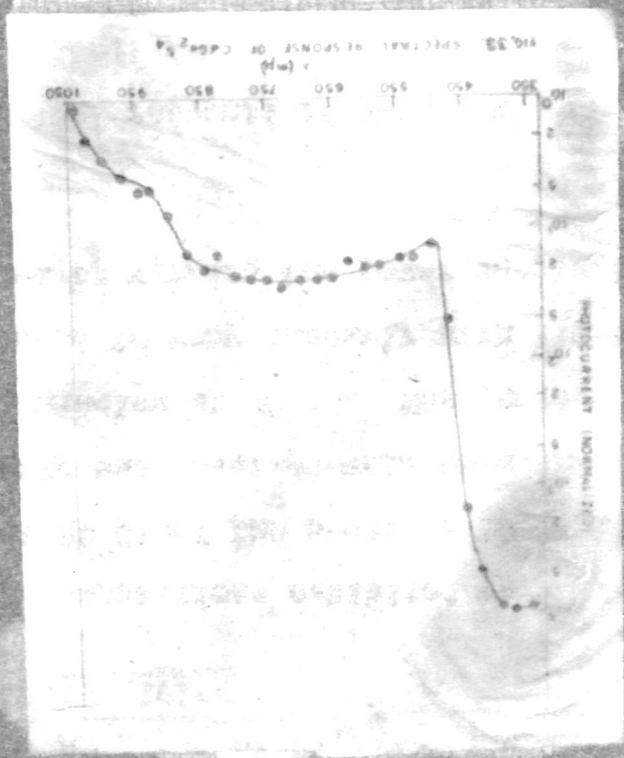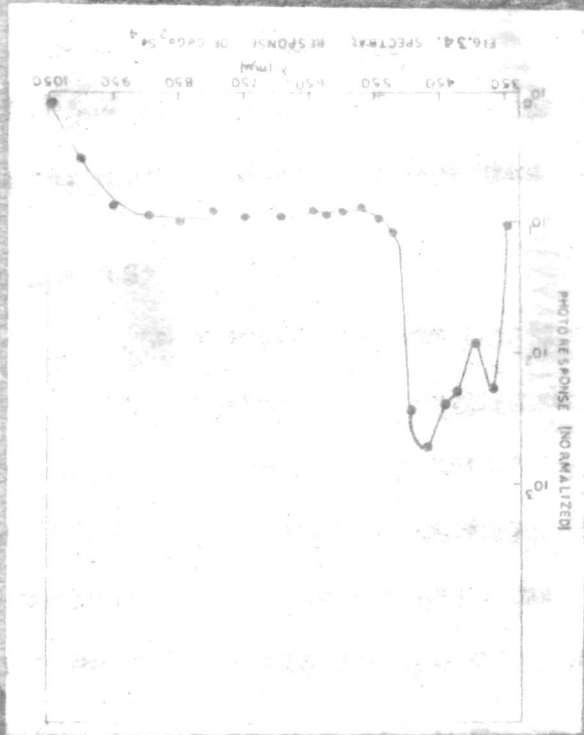
3.4 RESULTS OF SPECTRAL RESPONSE OF PHOTOCONDUCTIVITY

All the compositions exhibited very high dark resistivity (at 25°C) of the order of $10^{12} - 10^{13}$ ohm. cm. Photoconductivity was observed only when the In-Ga contacts were annealed at 300°C. The photoconductivity response was found to vary linearly with light intensity which was tested by varying the power supply to the tungsten lamp.

The spectral response of photoconductivity of $CdGa_2S_4$ (Fig. 33) had a narrow peak at 3.35 eV which corresponds to the optical band gap (viz. 3.25 eV). On the other hand photoconductivity spectrum of $CdGa_2Se_4$ (Fig. 34) exhibited peaks at 3.3 eV, 2.92 eV and 2.58 eV. The last peak may be attributed to the optical band gap (viz. 2.25 eV) whereas the peaks at 2.92 and 3.3 eV may be thought to arise from electronic transitions between the valence sub-bands and conduction band. Though the nature of the plots is in agreement with those of the Abdullaev et al.[30] the energy values observed by us are higher than theirs.

Photoconductivity spectra of the new compositions $CdGa_2S_3Se$, $CdGa_2S_2Se_2$ and $CdGa_2SSe_3$ are shown in Figs. 35, 36 and 37. In case of each spectrum there are two peaks
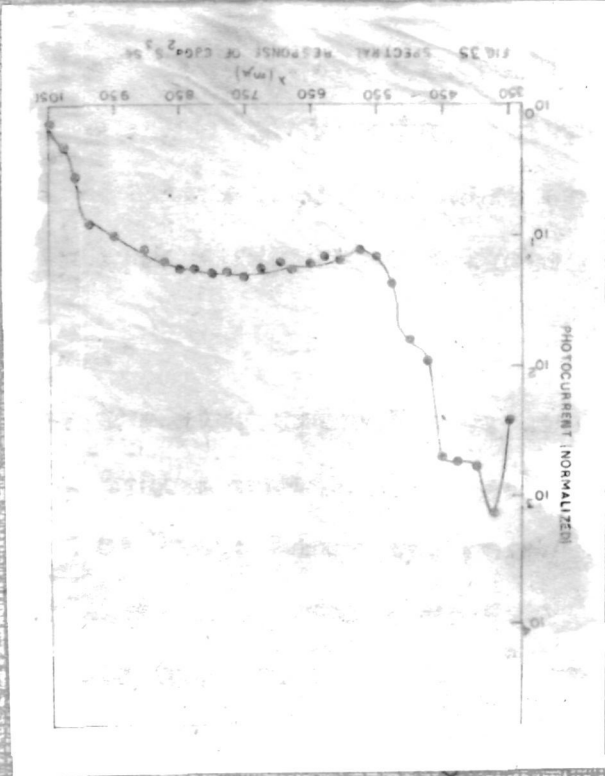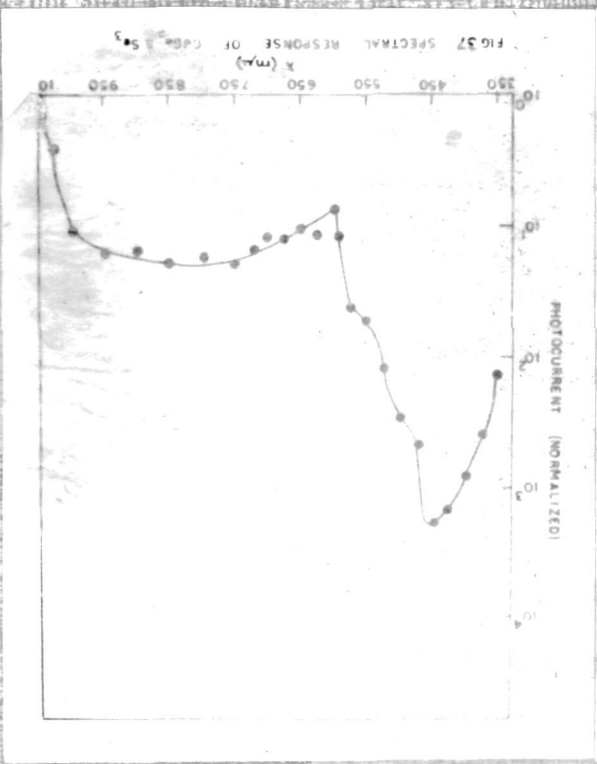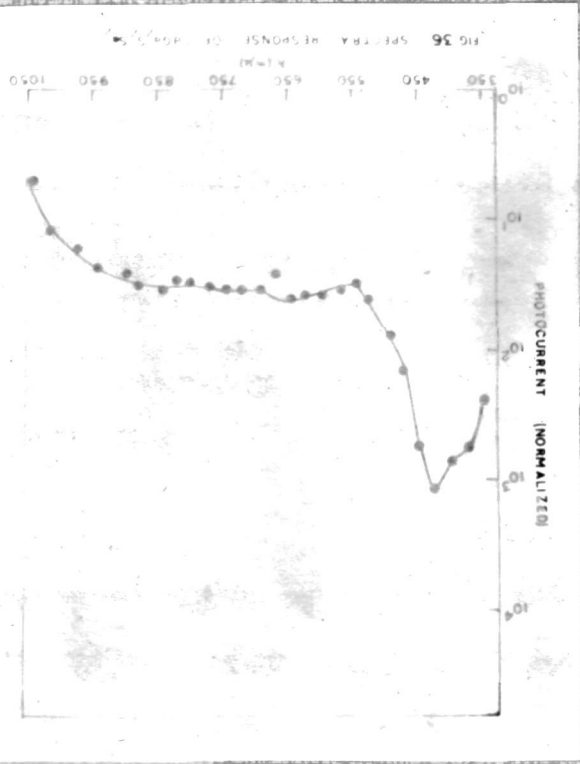
at higher energy side in addition to the one corresponding to the intrinsic minimum band gap. The values of the positions of these peaks are noted in Table-13. The appearance of higher energy peaks beyond the optical band gap indicates sub-band structure of the valence band of these compounds.

All samples exhibited a diffuse peak in photoconductivity spectrum from long wave side increasing from 1050 m μ to 850 m μ and remains overall constant upto 650 m μ and then decreasing to 550 m μ. Such a behaviour is characteristic of localized energy levels in the forbidden gap. Such energy states generally come from variety of defects. In the present case, they could arise from a small departure from stoichiometry or from position disorder arising from exchange of atoms between Cd and Ga sites.

TABLE - 13

Energy band gaps obtained from
photoconductivity curves

	Peak corresponding to E_g (optical)	Peak II	Peak III
$CdGa_2S_4$	3.35	----	----
$CdGa_2S_3Se$	3.03	----	2.53
$CdGa_2S_2Se_2$	2.85	3.27	2.48
$CdGa_2SSe_3$	2.70	3.18	2.07
$CdGa_2Se_4$	2.58	3.30	2.82

The long wave tail in the absorption spectrum may be attributed to this diffuse broad peak in photoconductivity spectra. The extrinsic defects which give rise to the diffuse absorption and the tail in the photoconductivity is probably responsible for the temperature independent part in the conductivity graph at low temperature ($< 200^\circ$C).

3.5 RESULTS OF ELECTRICAL CONDUCTIVITY MEASUREMENTS

The plots of log R vs 1/T for all these compositions are shown in Figs. 39-43. The electrical conductivity showed no change in the temperature range 25° to 250°C. It increased with temperature upto 300°C and more faster above 300° to 350°C. After cooling the sample to room temperature a set of readings was again recorded for the second run of heating from 25° to 350°C. The activation energy as calculated from the slope of log R vs 1/T plots matched with the half of the optical band gap for the first run, but was found to increase in the second run. Further increase in activation was also found when the set of readings was recorded third time while heating from 25° to 350°C. The various values of activation energy are recorded in Table-14 and plotted in Fig. 44.
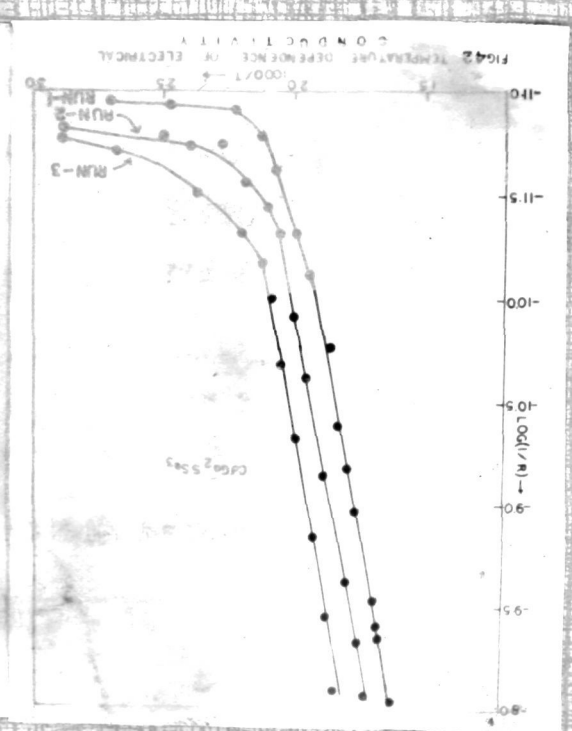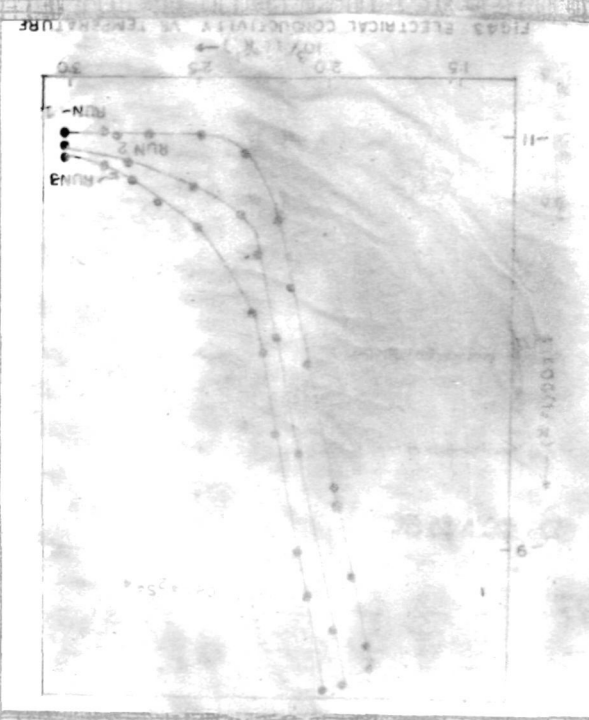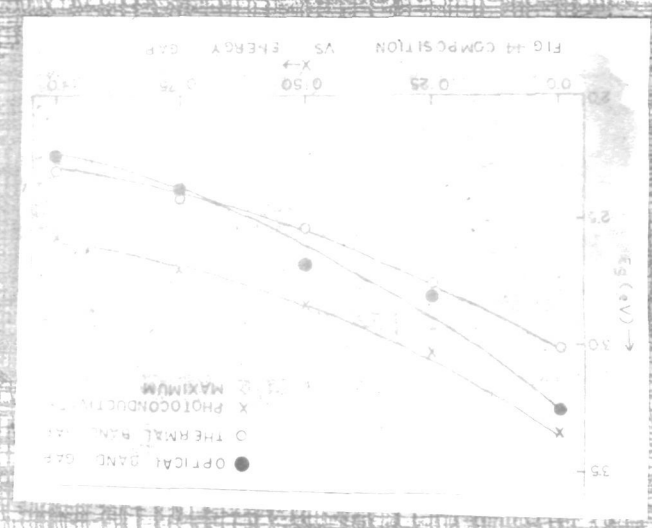
FIG 4.5 THERMOELECTRIC POWER vs TEMPERATURE

$10^3/T \ (^\circ K^{-1}) \rightarrow$

2.0

1.9

1.8

1.7

−800

−600

DEG

μV

−400

−200

CdIn$_2$S$_4$

FIG 4.4 COMPOSITION vs ENERGY GAP

$\leftarrow$ X

0.0   0.25   0.50

$E_g \ (eV) \rightarrow$

2.5

3.0

3.5

MAXIMUM
X PHOTOCONDUCTIVITY
O THERMAL BAND GAP
● OPTICAL BAND GAP

FIG 4.3 ELECTRICAL CONDUCTIVITY vs TEMPERATURE

$10^3/T \ (^\circ K) \rightarrow$

1.5   2.0   2.5   3.0

RUN-1
RUN-2
RUN-3

−11

LOG($1/R$) →

CdIn$_2$S$_4$

FIG 4.2 TEMPERATURE DEPENDENCE OF ELECTRICAL CONDUCTIVITY

$1000/T \rightarrow$

2.0   2.5   3.0

RUN-1
RUN-2
RUN-3

−14.0

−11.5

−10.0

LOG($1/R$) →

−10.5

−9.0

−9.5

−8.0

CdIn$_2$S$_3$

TABLE - 14

Activation energy values (eV)

Compound	Run I	Run II	Run III
$CdGa_2S_4$	1.508	1.648	1.738
$CdGa_2S_3Se$	1.390	1.528	1.662
$CdGa_2S_2Se_2$	1.270	1.385	1.655
$CdGa_2SSe_3$	1.200	1.290	1.360
$CdGa_2Se_4$	1.155	1.240	1.350

The most interesting feature of the electrical conductivity data is that the compounds in spite of their large band gaps exhibit intrinsic conduction in the temperature range $250-350^{\circ}C$. This shows that the extrinsic defects are indeed very small in these crystals.

3.6 RESULTS OF TEMPERATURE DEPENDENCE OF THERMOELECTRIC POWER

Simultaneously we studied the variation of thermoelectric power with temperature in the same temperature range. All the compositions exhibited n-type conduction. In the first run of heating cycle the thermoelectric power was found to decrease from approx. 400 $\mu V/deg.$ to 300 $\mu V/deg.$ In the second and third run of heating cycles

FIG.46 THERMOELECTRIC POWER VS TEMPERATURE

CdGa₂S₃Se

FIG.47 THERMOELECTRIC POWER VS TEMPERATURE

CdGa₂S₂Se₂

FIG.48 THERMOELECTRIC POWER VS TEMPERATURE

CdGa₂S₁Se₃

FIG.49 THERMOELECTRIC POWER VS TEMPERATURE

CdGa₂Se₄
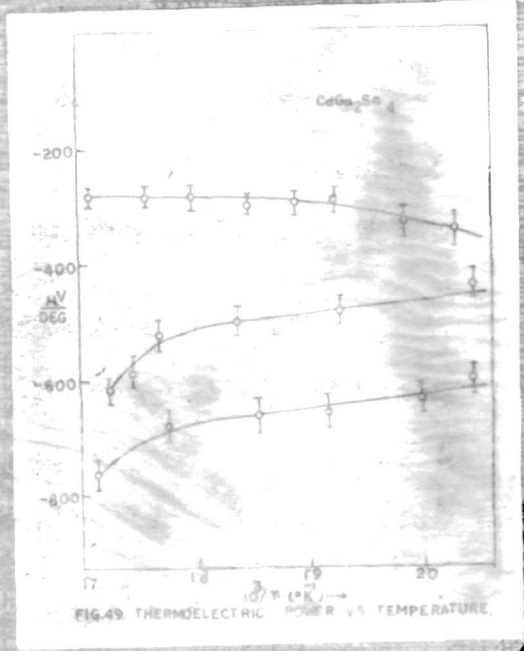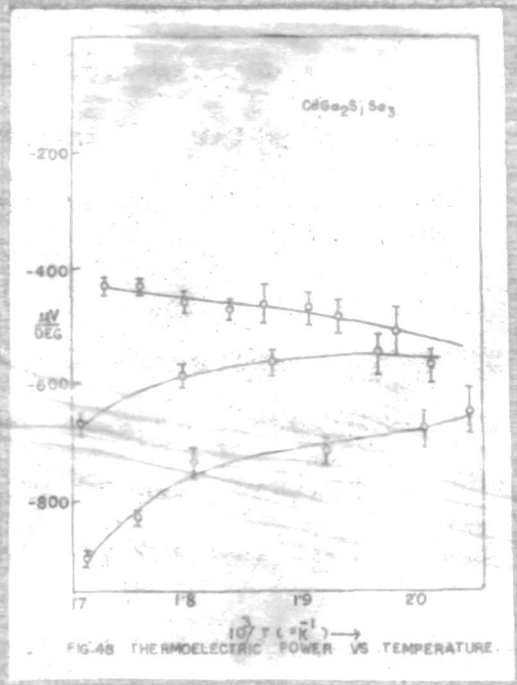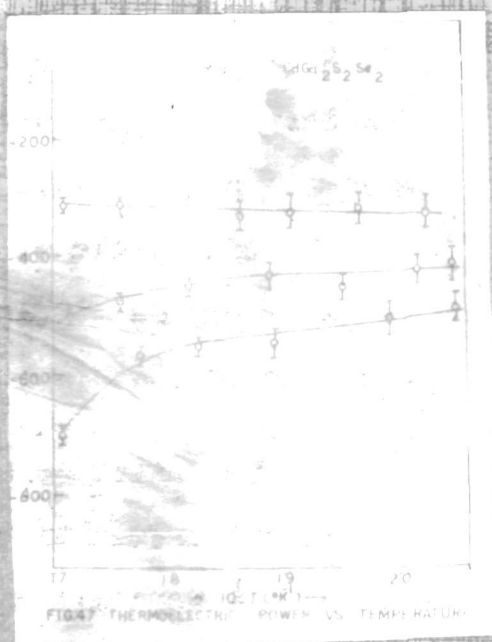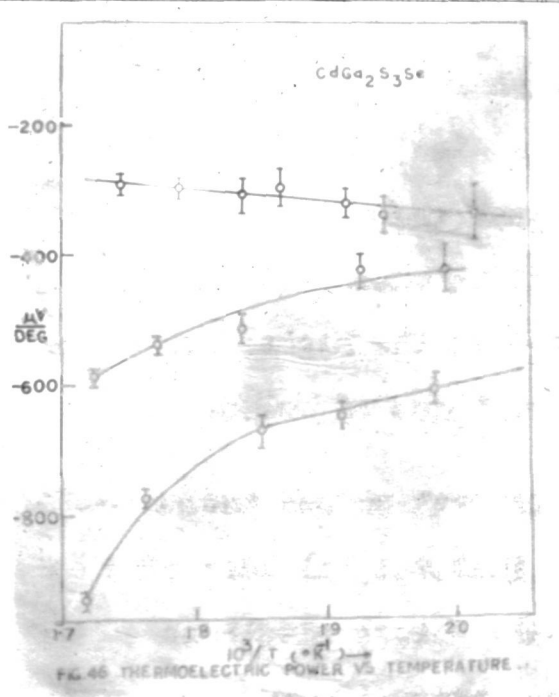
the thermoelectric power shows a marked increase with
temperature (Figs. 45-49). The small values of thermo-
electric power indicate that the samples are intrinsic
in the first cycle of heating whereas the negative sign
probably may be attributed to the higher values of
mobility of electrons than those of holes.

The variation of activation and thermoelectric power
may be attributed to two factors: (1) loss of S or Se
making the crystals to have excess electrons and
(2) diffusion of In or Ga making the crystals excess of
metal. Both these would increase with the temperature
and time. The first run of heating cycle then may be
assumed to give the effects of the intrinsic conduction,
whereas the second and third runs give the effects in
addition to the intrinsic of the loss of S and Se and
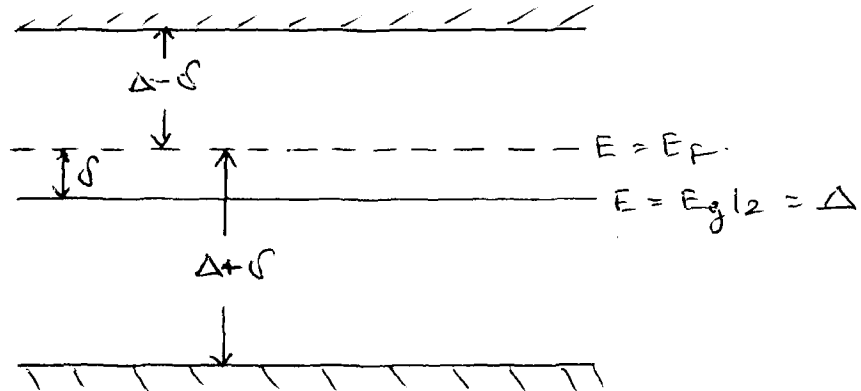diffusion of In and Ga.

The thermoelectric power vs temperature plots have
positive intercepts and negative slopes. This is intere-
sting and can be explained if we realize that we are
dealing with intrinsic sample in this temperature range.

Hence the thermoelectric coefficient θ is given
by

$$\theta = \frac{\sigma_e \theta_e + \sigma_h \theta_h}{\sigma_e + \sigma_h}$$

where $\quad \theta_e = -\dfrac{K}{e}\left[(5/2 - 3) + \dfrac{\Delta - \delta}{KT}\right]$

and $\quad \theta_h = \dfrac{K}{e}\left[(5/2 - 3') + \dfrac{\Delta + \delta}{KT}\right]$

where $\Delta = E_g/2$ and $\delta = E_F - E_g/2$. Hence the intercept is governed by the values of 3 and $3'$, whereas the slope mainly by δ. This can be illustrated by writing the above equations in a simplified form for a special case where $\tau_e = \tau_h$, as

$$\theta = \frac{\theta_e + \theta_h}{2} = \frac{K}{e}\left[(3' - 3) + \frac{2\delta}{KT}\right]$$

Small slope is indication of small δ i.e. the Fermi level is close to the center of the gap which is consistent with the intrinsic conduction.

*****

SUMMARY AND CONCLUSIONS

The compounds $CdGa_2S_4$ and $CdGa_2Se_4$ belong to the defect chalcopyrite (space group $I\bar{4}$) family. We have prepared a series of compounds $CdGa_2S_{4(1-x)}Se_{4x}$ and grown their single crystals by chemical transport reaction method.

A complete solid solubility was observed between these two compounds. The a-axis values varied linearly with composition while c-axis values initially showed a slower rise for $x < 0.5$ and then marked rapid rise with increasing selenium content.

Optimum conditions required for the growth of the crystals have been established. The crystals of $CdGa_2S_4$ and $CdGa_2S_3Se$ had the biggest face parallel to (001) plane whereas crystals of compounds $CdGa_2S_2Se_2$, $CdGa_2SSe_3$ and $CdGa_2Se_4$ were triangular prisms with a face parallel to (112) plane and $\angle 110 >$ as its growth axis.

The parameters x, y and z for selenium position in $CdGa_2Se_4$ were obtained by comparing the calculated values of F^2 factors with those obtained from observed intensities. The best match was found for $x = y = 0.25$ and $z = 0.15$.

The optical absorption spectra revealed that the fundamental absorption edge varies with the composition from 2.2 eV to 3.25 eV. The plots $(\alpha \hbar w)^2$ vs hw revealed that these compounds are direct band gap materials. The values of energy gaps were also deduced from spectral response (λ_{max}) measurements and found to be in agreement with those deduced from optical absorption measurements. D.C. resistivity vs temperature studies revealed that, in spite of their large band gaps, these compounds exhibit intrinsic semiconduction above the temperature of $250^{\circ}C$. The energy gap values matched with those obtained from other measurements. All the samples were n-type and had thermoelectric power approximately constant $\sim 300 \mu V/deg$. in the temperature range $250^{\circ}-350^{\circ}C$. However, the thermal dependence of electrical conductivity and thermoelectric power indicated strong irreversibility with thermal heating and cooling cycles. Such behaviour has been attributed to the diffusion of contact materials such as Ga and In.

Thin films of the compounds $CdGa_2Se_4$ and $CdGa_2S_4$ were prepared by vacuum evaporation and flash evaporation methods. Optical absorption spectra were studied in the visible range of radiation. Analysis of the absorption curve indicated close agreement with that of

the bulk material. The plots of α^2 **vs** ℏw yielded 2.51 eV and 3.50 eV as values of the energy gaps for direct transitions for the thin films of $CdGa_2Se_4$ and $CdGa_2S_4$ respectively.

*****

REFERENCES

R E F E R E N C E S

(1)   Willardson, R.R. and Beer, A.L., (Ed.),
        "Semiconductors and semimetals: Physics of
        III-V compounds", Vol. 1,2,3 and 4, Academic Press,
        N.Y. and London, 1966.

        Aven, M. and Prener, J.S., "Physics and Chemistry
        of II-VI Compounds", North Holland Publishing Co.,
        Amsterdam, 1967.

(2)   Grimm, H.G. and Sommerfeld, A., Z. Phys.,
        1926, 36, 36.

(3)   Goodman, C.H.L., J. Phys. Chem. Solids, 1958,
        6(4), 305.

(4)   Goryunova, N.A., "Chemistry of diamond-like semi-
        conductors", Chapman and Hall, London, 1965.

(5)   Hobden, M.V., Nature, 1968, 220(5169), 781.

(6)   Levine, B.F., Bethea, C.G. and Kasper, H.M.,
        IEEE J.Q. Electron, 1974, Q.E 10, 904.

(7)   Abdullaev, G.V., Agaev, V.G., Antonov, V.B.,
        Nani, R.Kh. and Salaev, E.Yu., Sovt. Physics
        Semicond., 1972, 6(9), 1492.

(8)   Hahn, H., Frank, G. Klingler, W., Storger, A.D.
        and Storger, G., Z. anorg. Chem., 1955, 279, 241.

(9)   Antonov, V.B., Guseinov, G.G., Guseinov, D.T. and
        Nani, R.Kh., Dokl. Akad. Nauk Azerb SSR, 1968,
        24(8), 12 (Russ).

(10)   Hobden, M.V., Acta Crystallogr. (A), 1969, 25, 633.

(11)   Mamedov, K.K., Aliev, M.M., Kerimov, I.G. and
        Nani, R.Kh., Phys. Stat. Solidi (A), 1972, 9(2),
        K149.

(12)   Nitsche, R., Bolsterli, H.U. and M. Lichtensteiger,
        J. Phys. Chem. Solids, 1961, 21, 199.

(13) Beun, J.A., Nitsche, R. and Lichtensteiger, M.,
      Physica, 1961, 27, 448.

(14) Shand, W.A., J. Cryst. Growth, 1969, 5(3), 203.

(15) Chedzey, H.A., Marshall, D.J., Parfitt, H.T. and
      Robertson, D.S., J. Phys. (D), 1971, 4(9), 1320.

(16) Kyropolus, S., Z. anorg. Chem., 1926, 154, 308.

(17) Cockayne, B., Robertson, D.S. and Bardsley, W.,
      Brit. J. Appl. Phys., 1964, 15, 1165.

(18) Mullin, J.B., Straughan, B.W. and Brickell, W.S.,
      J. Phys. Chem. Solids, 1964, 26, 782.

(19) Stemple, N.R. and Suchow, R., J. Electrochem. Soc,
      1964, 111, 191.

(20) Austin, I.G., Goodman, C.H.L. and Pengelly, A.E.,
      J. Electrochem. Soc., 1956, 103, 609.

(21) Abdullaev, G.B., Guseinova, D.A., Kerimova, T.G.
      and Nani, R.Kh., Fiz Tekh. Poluprov., 1973,
      7(4), 840 (Russ).

(22) Kolosenki, S.M. and Tyrziu, M.P., Issled. Slozhnykh
      Poluprov., 1970, 112.

(23) Tyrziu, M.P. and Tyrziu, V.G., Izv. Akad. Nauk.
      SSSR, Neorg. Mater., 1971, 7(10), 1855 (Russ).

(24) Agaev, V.G., Antonov, V.B., Nani, R.Kh., and
      Salaev, E.Yu., Dokl. Akad. Azerb. SSR, 1970, 26, 8.
      (Russ).

(25) Strel'tsov, L.N., Chernykh, V.Ya. and Petrov, V.M.,
      Fiz. Tekh. Poluprov., 1967, 1(5), 793 (Russ).

(26) Abdullaev, G.B., Agaev, V.G., Antonov, V.B., Nani,
      R.Kh., and Salaev, E.Yu., Fiz. Tekh. Poluprov.,
      1971, 5(11), 2132 (Russ.)

(27) Gilevich, M.P. and Laevskaya, G.A., Vestn. Beloruss.
      Univ., 1972, 2(2), 3 (Russ.).

(28) Radautsan, S.I., Zhitar, V.F. and Railyan, V. Ya.,
      Izv. Akad. Nauk. Mold SSR. Sev. Fiz. Tekh. Mat. Nauk,
      1973 (3), 41 (Russ.).

(29)   Fochs, P.D., Proc. Phys. Soc. (London), 1956,
       B-69, 70.

(30)   Radautsan, S.I. Zhitar, V.F., Kosnichan, I.G.
       and Shmiglyuk, M.I.,   Fiz. Tekh. Poluprov.,
       1971, 5(11), 2240 (Russ).

(31)   Abdullaev, G.B., Agaev, V.G., Antonov, V.B., Nani,
       R.Kh., and Salaev, E.Yu.,   Fiz. Tekh. Poluprov.,
       1972, 6(9), 1729 (Russ.).

(32)   Abdullaev, G.B., Agaev, V.G., Antonov, V.B.,
       Mamedov, A.A., Nani, R.Kh. and Salaev, E.Yu.,
       Fiz. Tekh. Popuprov., 1973, 7(6), 1051 (Russ.).

(33)   Whelan, J.M. and Wheatley, G.H.,   J. Phys. and
       Chem. Solids, 1958, 6, 169.

(34)   Willardson, R.K. and Goering, H.L., (Eds.),
       "Compound Semiconductors", Vol. 1, preparation
       of III-V compounds, Reinhold, N.Y., 1962.

(35)   Luzhnaya, I.,   Izv. Akad. Nauk. Neorg. Mater.,
       1966, 2, 128.

(36)   Ray, B., "II-VI Compounds", Pergamon Press, 1969.

(37)   Vaipolin, A.A. and Korshak, N.M.,   Physics
       (Proc. 23rd Sci. Conf. at Leningrad Structural
       Engineering Institute), Leningrad, 1965, p.47.

(38)   San-MeiKu, J. Electrochem. Soc., 1963, 110, 991.

(39)   Spring-Thorpe, A.J. and Pamplin, B.R., J. Crystal
       Growth, 1968, 3-4, 313.

(40)   Robbins, M. and Lambrecht, V.G. Jr., Mater. Res.
       Bull, 1973, 8(6), 703.

(41)   Finch, G.I. and Wilman,   Erg. Exakt. Naturav,
       1937, 16, 353.

(42)   Bardeen, J.,   Phys. Rev., 1947, 71, 717.

(43)   Schwarz, R.F. and Walsh, J.F.,   Proc. IRE, 1953,
       41, 1715.

(44)   Borneman, E.H., Schwarz, R.F. and Stikler, J.J.,
       J. Appl. Phys., 1955, 26, 1021.

(45)   Wurst, E.C.(Jr.), and Borneman, E.H.,   J. Appl.
       Phys., 1957, 28, 235.

(46)   Henish, H.K.,   "Rectifying Semiconductor Contacts"
       Oxford University Press, N.Y., 1957.

(47)   Harman, G.G. and Higier, T.,   J. Appl. Phys.,
       1962, 33, 2198.

(48)   Michaelson, H.B.,   J. Appl. Phys., 1950, 21, 536.

(49)   International Tables for X-ray Crystallography.

(50)   Zlatkin, L.B. and Ivanov, E.K.,   J. Phys. Chem.
       Solids, 1971, 32, 1733.

(51)   Antonov, V.B., Dzhuraev, N.D. and Nani, R.Kh.,
       Dokl. Akad. Nauk. Azerb. SSR, 1973, 29(3), 8 (Russ.)

(52)   Chaldyshev, V.A. and Pokrovskii, V.N., Izv. Vuz.
       USSR Fiz., 1960, 2, 173. ibid, 1963, 5, 103;

       Karavaev, G.F. and Poplavnoi, A.S., Sovt. Phys.
       Solid State, 1967, 8, 1704.

       Karavaev, G.F., Poplavnoi, A.S. and Chaldyshev,
       V.A.,   Sovt. Phys. Semicond., 1968, 2, 93.

(53)   Radautson, S.I., Zhitar, V.F., Kosnichem and
       Shmiglyuk, M.I., Fiz. Tekh. Poluprov., 1971, 5, 2240.

(54)   Heine, V., "Group Theory in Quantum Mechanics",
       Pergamon Press, London (1960).

(55)   Eby, J.E., Teegardeen, K.J. and Dutton, D.B.,
       Phys. Rev., 1959, 116, 1099.

(56)   Sussmann, R. and Cardona, M.,   Bull. Amer. Chem. Soc.,
       1966, 11, 85.

(57)   Cardona, M. and Greenway, D.L.,   Phys. Rev.,
       1964, 133A, 1685.

(58)   Greenway, D.L. and Harbeke, G.,   J. Phys. Chem.
       Solids, 1965, 26, 1585.

(59)   Tsukahara, J., Satoh, T. and Tsushima, T.,
       J. Cryst. Growth, 1974, 24-25, 158.

(60)   Cardona, M. and Sommers, H.S. (Jr), Phys. Rev.,
       1961, 122, 1382.